

Institut Supérieur de l'Aéronautique et de l'Espace



Structural Optimization of a
Flexible Wing:
Parametric Model Approach

Projet de Fin d'Etudes / Final Year's Thesis

July 2011

HABIB ISSA MATTOS Francisco (ISAE Supaero / ITA)

Prof. Dr. Joseph MORLIER (ISAE / DMSM)

Abstract

The following work presents a parametric model approach for the optimization of a flexible wing aiming the improvement of the reduced model developed in parallel to this study. At first, how to create a complex metallic Wing-Box model for single aisle commercial aircrafts is demonstrated, following what big manufactures such as Airbus and Boeing use in theirs products, and developing a full parametric PCL code in Patran. Then, an optimization processes is presented using the Nastran Design Sensitivity and Optimization algorithm, also known as Sol200.

The main objective is to optimize the global structure weight respecting all structural criteria and constraints, and using the spars and skin thickness as design variables. After the optimization, the importance of upper and lower skins is minimized and almost all efforts are concentrated on spars, specially the rear spar. It's also shown that the strain criterion is stronger than the stress one, which considers shear and buckling as the critical design points, although fatigue is also relevant when designing the lower Wing-Box Skin.

This computational model allows the determination of all Wing-Box element thickness that give the minimum wing weight, helping the preliminary design task to achieve the optimized structure in the shortest time, enhancing the results by the lowest costs possible. Associating this work with an aerodynamic approach using CFD would make possible to create a variation of the required profile to construct the real wing that, when deformed, would assume its best shape in terms of aerodynamics, still respecting all structural constraints and minimum weight possible. Finally, another important approach consists of doing the exactly same study but with composite materials, since the future of aviation may reside no more in metallic alloys, but in composites.

Table of Contents

TABLE OF VARIABLES AND CONSTANTS	5
1 - INTRODUCTION	7
1.1 - DMSM ISAE / SUPAERO	8
1.2 - INTERNSHIP OBJECTIVES.....	9
1.3 - NASTRAN OPTIMIZATION	9
2 - MODEL AND DEVELOPMENT	10
2.1 - PATRAN	11
2.1.1 - <i>Wing Geometry</i>	12
2.1.2 - <i>Materials</i>	16
2.1.3 - <i>Properties</i>	16
2.1.4 - <i>Boundary Conditions</i>	19
2.1.5 - <i>Load Case</i>	19
2.1.6 - <i>Meshing</i>	25
2.2 - NASTRAN	26
2.2.1 - <i>Sol200</i>	29
2.2.2 - <i>Analysis</i>	31
2.2.3 - <i>Design Variables</i>	31
2.2.4 - <i>Criteria and Constraints</i>	32
2.2.5 - <i>Design Optimization Parameters</i>	34
3 - RESULTS	36
3.1 - NON-OPTIMIZED WB (PART I).....	37
3.2 - WB OPTIMIZED BY STRESS CRITERIA ONLY (PART II).....	39
3.3 - WB OPTIMIZED BY STRESS, STRAIN AND MAX. DISPLACEMENT CRITERIA (PART III)	48
4 - CONCLUSION	57
5 - REFERENCES	59
ANNEX 1 - MORE OPTIMIZATION RESULTS FOR PART II (8 NACA PROFILES)	62
ANNEX 2 - NUMERICAL RESULTS FOR PART II OPTIMIZATION	67
ANNEX 3 - NUMERICAL RESULTS FOR PART III OPTIMIZATION	71
ANNEX 4 - HOW TO USE THIS WORK / DOCUMENTATION TUTORIAL.....	75

Table of Variables and Constants

g_j	Inequality Constraints
h_k	Equality Constraints
x_i	Side Constraints
X	Design Variables
b	Wingspan
S	Wing Area
AR	Aspect Ratio
λ or ϵ	Taper Ratio
δ	Dihedral
A	¼ Chord Sweep
θ	Wing Tip Torsion
<i>MTOW</i>	Maximum Takeoff Weight
m	Maximum Camber
p	Maximum Camber Position
t	Maximum Relative Thickness
E	Young's Modulus
ν	Poisson Ratio
ρ	Density
T_i	Cartesian Translation (i= x, y or z coordinate)
R_i	Cartesian Rotation (i= x, y or z coordinate)
n_z	Critical Load Factor
n_{zce}	Extreme Load Factor
C_m or $C_{mprofil}$	Profile Moment Coefficient
Y	Normalized Position along Spanwise
L	Total Lift
V_a	Aerodynamic Speed
C_z	Lift Coefficient
g	Gravity Acceleration
$S(Y)$	Total Shear Force
$S_a(Y)$	Shear Force due to Aerodynamic Efforts
$S_m(Y)$	Shear Force due to Inertial Efforts
$B(Y)$	Total Bending Moment

$B_a(Y)$	Bending Moment due to Aerodynamic Efforts
$B_m(Y)$	Bending Moment due to Inertial Efforts
$T(Y)$	Total Torsion
$T_a(Y)$	Torsion due to Aerodynamic Efforts
$T_m(Y)$	Torsion due to Inertial Efforts
C	Local Chord
C_r	Root Chord
M_{wing}	Wing Mass
M_{fuel}	Fuel Mass
M_{mot} ou M_m	Engine Mass
Y_m	Engine Position along Spanwise
l_{CG_CS}	Distance between Gravity Center and Shear Center
d_F	Vertical Distance between Engine Center of Thrust and Shear Center
d_M	Horizontal Distance between Engine Center of Mass and Shear Center
F	Engine Thrust
σ_{comp}	Compression Stress
$(\sigma_{comp})_{cr}$	Critical Compression Stress
τ_{xy}	Shear Stress
$(\tau_{xy})_{cr}$	Critical Shear Stress
η_s and η_c	Plasticity Reduction Factor
K_s	Buckling Coefficient due to Shear
K_c	Buckling Coefficient due to Compression
t	Thickness
t_s	Thickness for Local Buckling
f_{ty}	Maximum Distortion Energy Yield
σ_{vm}	Von Misses Stress
d_{ytip}	Wing Tip Displacement
ε	Strain

1 - Introduction

This Final Year's Thesis is intended to give a parametric approach to a flexible wing optimization for the Osycaf Project. This entire study is directly correlated to the reduced model developed by Assis Lima [1], which provides the inputs and post-processing for the results of this work, by its Surrogate Model.

The main objective is to structurally optimize a Wing-Box for commercial aircrafts, providing the lowest weight for the entire structure that resists to all loadings and boundary conditions, respecting the parameters constraints and conditions that define a real wing, according to manufactures such as Airbus, Boeing, Embraer and Bombardier.

To create the Wing-Box, PCL code was used as default, with the help of MSC Patran 2007, which consists of a strong GUI tool to design complex structures to be after analyzed in Nastran. The first part is then to create the wing based on parameters such as span, chord sweep, taper ratio, tip torsion, dihedral and a given profile. This is extremely important to allow changing the entire wing just by changing the parameters and running the PCL code once more, without the need to reconstruct everything from the beginning.

After this, the boundary conditions are implemented, as well as the loading case that is based on complex aerodynamics and inertial models. The geometry is then meshed and materials and properties added, generating a modeled structure ready to be exported as bulk data by Patran to Nastran.

With all elements generated, the optimization process starts using Sol200 in Nastran, a Design Sensitivity and Optimization algorithm. The Executive Control deck is defined as well as the Case Control Deck and the Bulk Data. In this moment, the stress, strain and displacement criteria are added and the constraints applied. The variables are chosen and the optimization parameters adjusted.

Running Sol200, the optimized Wing-Box configuration is returned in terms of thickness of every section of the Wing-Box spars and skins. The global weight is the objective design for minimization and the new wing presents the lightest configuration that respect all structural criteria and constraints, keeping wing geometry, properties and materials.

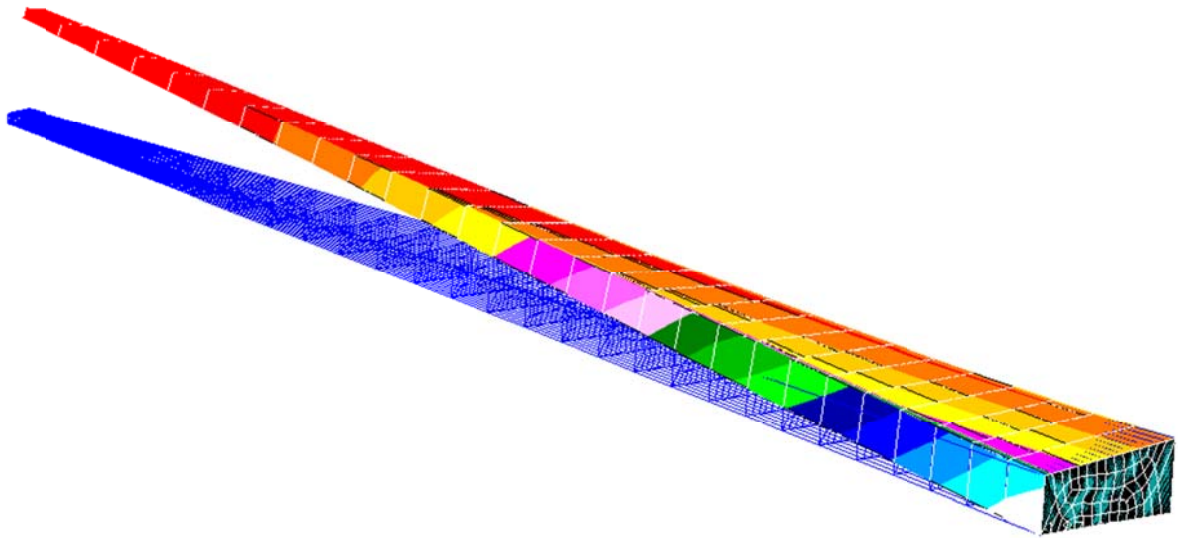


Figure 1 - Final Wing-Box NACA 2420 model in static analysis - displacement translational.

1.1 - DMSM ISAE / Supaero

The Department of Structural Mechanics and Materials of the Superior Institute of Aeronautics and Space (DMSM/ISAE), in Toulouse - France, focus on researching and developing methods and tools for design of aerospace structures, and meets best the needs of industry by its 4 axes: Damage of Composite Aerospace Structures, Fatigue of Metallic Materials and Structures, Vibratory Dynamics and Advanced Numerical Methods for Mechanics.

DMSM also covers the scientific disciplines related to solid mechanics including the core subjects of general mechanics and continuum for Supaero and Ensica academic formations. Structures, particularly the thin ones, are the subject of development in static, dynamic and thermal analysis, leading one hand on the certification of aerospace structure and secondly the use and qualification of metallic structural materials and composite structural components.

1.2 - Internship Objectives

One of the objectives of this internship is providing a reasonable approach to structural modeling in Patran and optimization and design sensitivity in Nastran. This research and development aim to be a direct response for the reduced model also proposed by the same project. In this way, the numerical optimization results shall be used to validate and improve the analytical equations developed for preliminary design of future aircraft programs. It is important to remember that even numerical solutions are still expensive, and reducing costs is fundamental for competitive industries.

Another objective is to provide all tools and academic support for a Final Year's Thesis, which represents the last step on an engineering graduation program. The parametric approach and structural optimization using Sol200, on the other way, represents only a small part in a much bigger project named Osycaf. This program started on April 2010 and goals the optimization of a coupled fluid-structure representing a flexible wing - structural and aerodynamics optimization, in other words. The Osycaf Project is a partnership between ONERA, ISAE, IMT, CERFACS and STAE Toulouse.

1.3 - Nastran Optimization

The Sol200 is the Design Sensitivity and Optimization algorithm for Nastran based on gradient methods and used in this study. To understand its functioning, a few concepts must be established. The basic optimization problem statement is usually to find X that minimizes, or maximizes, the $F(X)$ objective subjected to:

$$g_j(X) \leq 0 \quad j = 1, \dots, n_g \quad \text{inequality constraints} \quad (1)$$

$$h_k(X) = 0 \quad k = 1, \dots, n_k \quad \text{equality constraints} \quad (2)$$

$$x_i^L \leq x_i \leq x_i^U \quad i = 1, \dots, n \quad \text{side constraints} \quad (3)$$

$$X = \{x_1, x_2, \dots, x_n\} \quad \text{design variables} \quad (4)$$

In this notation, items that are in upper case are vectors while members of the vectors are designated using a lower case symbol with a subscript to indicate the member.

The objective function is the scalar quantity to be minimized. It is a function of the set of design variables. Side constraints are placed on the design variables to limit the region of search. The inequality constraints are expressed in a less than or equal to zero form by convention, that is, a constraint is satisfied if its value is negative. Equality constraints, if present, must be satisfied exactly at the optimal design. The objective and constraint functions may either be linear or nonlinear functions of the design variables.

2 - Model and Development

The objective of this study is the optimization of a Wing-Box composed by ribs, front spar, rear spar, upper skin, lower skin, corner stiffeners and skin stringers. It's a Wing-Box based on commercial metallic wing, similar to those found in aircrafts such as Airbus A320 Family or Boeing 737 Family. But for the study, a totally parametric wing is desired since the profile will be changed many times and this implies on a lifting coefficient change, which will consequently change the wing area (and so the span) to keep total lift.

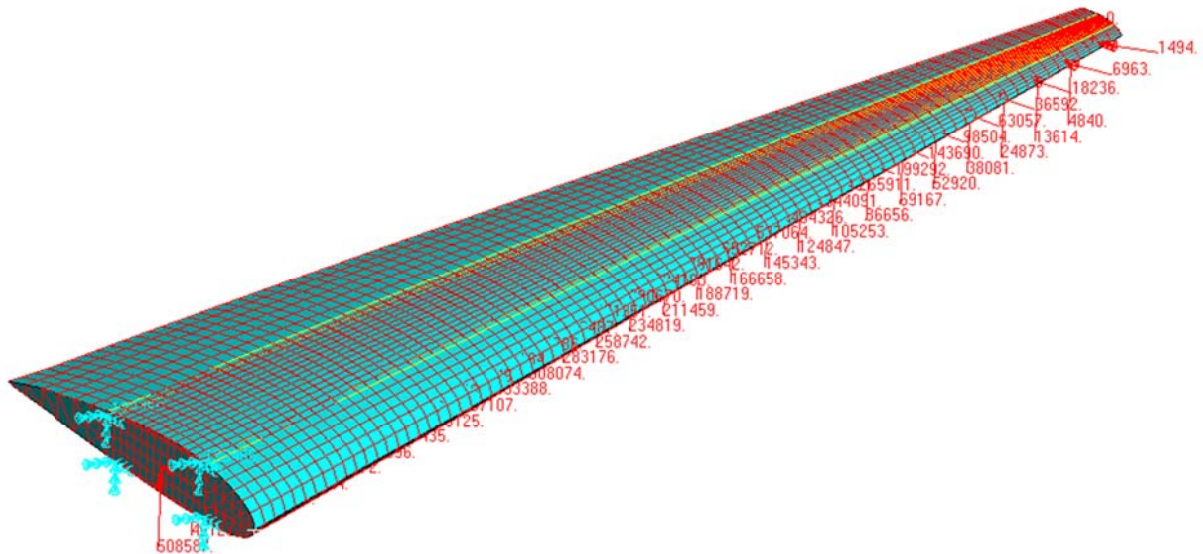


Figure 2 - Complete NACA 2415 wing model ready for analysis.

Initially a complete wing was created, including its skin. For the final study, though, the wing skin was suppressed so the model represents exactly what is proposed by the reduced model.

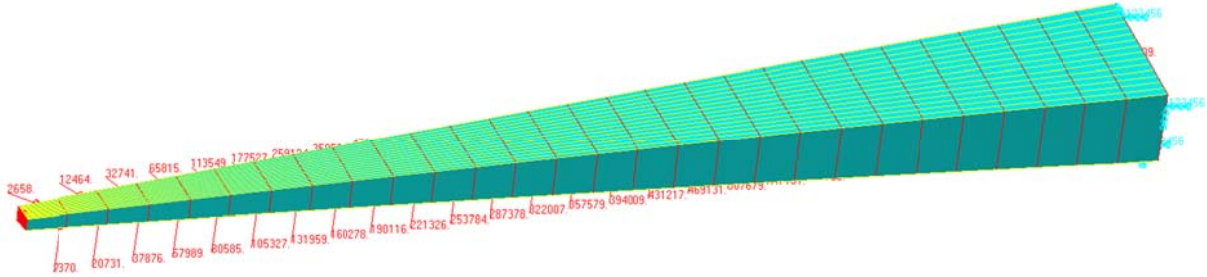


Figure 3 - Final Wing-Box NACA 2420 model ready for analysis.

2.1 - Patran

Patran is the world's most widely used pre/post-processing software for Finite Element Analysis (FEA), providing solid modeling, meshing, and analysis setup for MSC Nastran, Marc, Abaqus, LS-DYNA, ANSYS and Pam-Crash. For this study, MSC Patran 2007 was used as GUI interface for Nastran.

To define a wing 1 dimensional + 5 non-dimensional parameters and the cross section, known as the profile, are needed. The inputs are, then:

- Wingspan (b) or Wing Area (S)
- Aspect Ratio (AR)
- Taper Ratio (λ)
- Dihedral (δ)
- $\frac{1}{4}$ Chord Sweep (Λ)
- Wing Tip Torsion (θ)
- Profile (NACA 4-Digits Series)

It's also necessary to define the materials and the properties in the wing. In this study, two different types of aluminum are the materials chosen and for the properties shell and beam elements will be used. For the boundary conditions, a fixed wing – cantilever – is adopted. The static load is chosen to be the maneuver loading case and concerns aerodynamics, propulsion and inertial forces and moments.

The entire wing is constructed using PCL code. This is extremely important to compile a reusable session that can be run by Patran to reconstruct the model after changing just some

parameter - variable declaration. The code has more than 16.000 lines, and was programed with aid of macros in Microsoft Excel. Running the session to create geometry, loadings, boundary conditions, properties, materials and meshing takes no more than 8 minutes.

As mentioned, a complete wing was programed at first - complete Wing-Box and wing skin. For the study, the wing skin was suppressed, so that the structure is exactly the same studied in the reduced model, which is just the Wing-Box. This also gives a lighter model to be processed since the wing skin contains a great number of nodes and elements. After the session is finalized, the numerical model is converted to Nastran language by Patran, in a .blk file.

2.1.1 - Wing Geometry

The wing desired is based on some design restrictions. The first one is that the profile will be the same along the entire wing - constant profile cross section. The second one is the number of ribs, fixed to 29 and equally spaced. This means 28 wing sections, with a medium distance between ribs kept to around 0.6m / 2.0 ft, which is the medium distance adopted by Airbus and Boeing for almost all of theirs airplanes. The third is that wing torsion is considered to be linearly distributed along span.

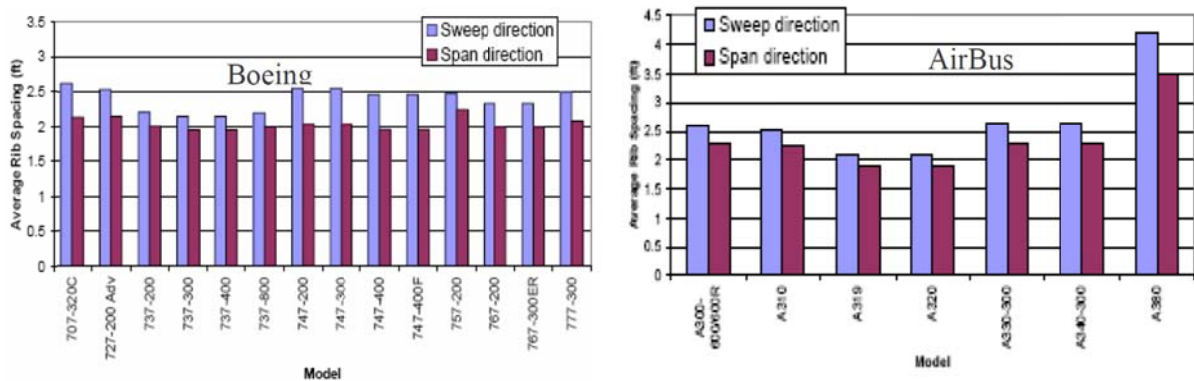


Figure 4 - Spacing of ribs in civil transport wings - Boeing and Airbus [17].

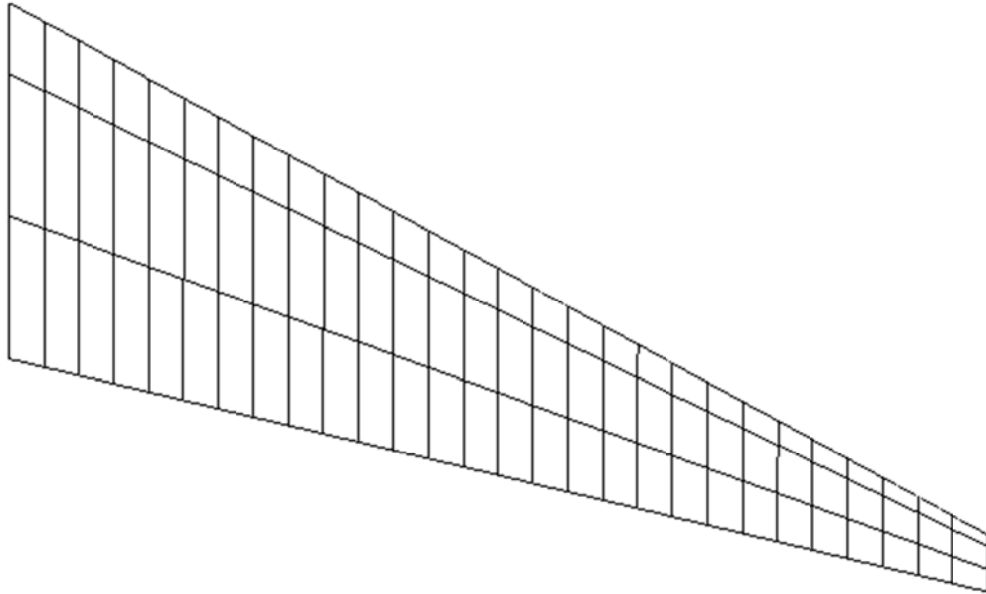


Figure 5 - Wing composed by 29 ribs equally spaced.

In this project some parameters were fixed to allow a deeper study on the influence of profile changing in the global structure. The non-dimensional parameters were kept constant, to be known:

- Aspect Ratio = 9.5
- Taper Ratio = 0.16
- Dihedral = +5°
- $\frac{1}{4}$ Chord Sweep = 25°
- Wing Tip Torsion = -3°

Some of the aircraft characteristics were also fixed:

- MTOW = 55000 Kg
- Fuel Mass = 18000 Kg (total)
- Engine Mass = 2500 Kg (each)
- Engine Thrust = 18415.9 N (each)

The wing area / wing span must attend the total lift required that is a function of the MTOW when in constant height flight - cruise. But total lift is also a function of the profile lift coefficient, which is different for each profile. In this way, the profile was chosen to be the variable, and defining the profile implies in a correspondent wing area / wing span, the only dimensional parameter. For this class of airplanes (MTOW around 55000 Kg), total wing span goes around 32 meters, so even very different airfoils should stay around this value.

For the profile and objective of this study, the NACA 4-Digits Series was chosen since its analytical equations allow inserting the entire profile as a variable when programing. This NACA Series has 3 parameters:

- Maximum camber (m)
- Maximum camber position (p)
- Maximum relative thickness (t)

The NACA 4-Digits Series equations are:

$$y_c = \frac{m}{p^2} (2px - x^2) \text{ from } x = 0 \text{ to } x = p \quad (5)$$

$$y_c = \frac{m}{p^2} [(1 - 2p) + 2px - x^2] \text{ from } x = p \text{ to } x = C \quad (6)$$

$$\pm y_t = \frac{t}{0.2} (0.2969\sqrt{x} - 0.1260x - 0.3516x^2 + 0.2843x^3 - 0.1015x^4) \quad (7)$$

$$x_U = x - y_t \sin \theta \quad (8)$$

$$y_U = y_c + y_t \cos \theta \quad (9)$$

$$x_L = x + y_t \sin \theta \quad (10)$$

$$y_L = y_c - y_t \cos \theta \quad (11)$$

$$\theta = \tan^{-1} \left(\frac{dy_c}{dx} \right) \quad (12)$$

The NACA 4-Digits Series also has a special notation: NACA ABXX has A for the maximum camber in %; B is for maximum camber position in % times 10; XX is for maximum relative thickness in %, about the chord. For example, a NACA 2412 means 2% maximum camber, 40% maximum camber position and 12% of maximum relative thickness.



Figure 6 - Examples of NACA 4-Digits Series automatically generated in Patran.

With these equations, 40 points were generated for upper camber and 40 for lower camber and after, these points were splined to create the profile contour. It was defined that the front spar would be at 20% of chord length, and the rear spar at 60%. This means that the Wing-Box is 40% of chord length in each section of the wing, and this measure is kept constant.

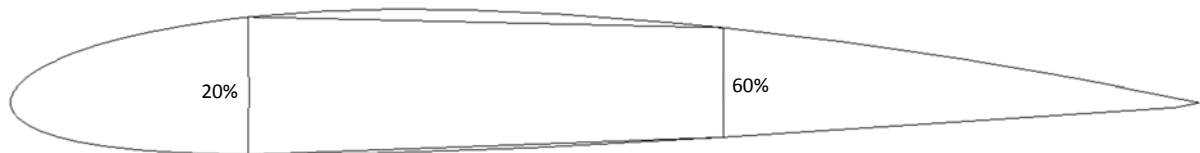


Figure 7 - Wing-Box spars located at 20% and 60% of local chord.

With the basic profile, it is now possible to start the wing creation. For each of the 29 ribs, the basic profile was scaled, translated and rotated, accordingly to aspect ratio, taper ratio, chord sweep, dihedral and torsion, respecting so every single dimension and spatial disposition. With all ribs, lines to support the stringers and stiffeners are created, so a complete frame is ready to give support to all the rest of the geometry. Surfaces are the next step, and they are created from the edge curves or from trimmed curves.

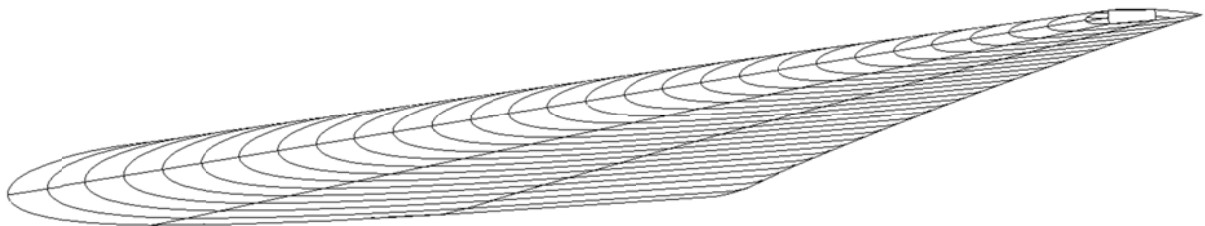


Figure 8 - Complete wing geometry generated by parametric PCL code in Patran.

2.1.2 - Materials

The materials adopted are the same usually found in metallic single aisle aircrafts of the big manufacturers. In this study, they are the aluminum alloys Al 7150 T7751 and Al 2024 T351 Bare, with homogeneous and isotropic properties, so Young's modulus (E), Poisson ratio (ν) and density (ρ) are the 3 parameters that matters - the Shear modulus G is computed directly from the equation $E = 2 \cdot (1 + \nu) / G$. The Al 7150 T7751 is used in the upper Wing-Box skin, upper corners stiffeners and upper Wing-Box skin stringers. The Al 2024 T351 Bare is used in the lower Wing-Box skin, lower corners stiffeners, lower Wing-Box skin stringers, front spar, rear spar and ribs. The properties are:

- Al 7150 T7751: $E = 71.016$ GPa, $\nu = 0.3$ and $\rho = 2823$ Kg/m³.
- Al 2024 T351 Bare: $E = 73.774$ GPa, $\nu = 0.3$ and $\rho = 2768$ Kg/m³.

Nastran translate these materials in the form of MAT1 that defines the material properties for linear isotropic materials.

2.1.3 - Properties

When studying a Wing-Box, buckling, shear and bending stress are important to be analyzed. In this way, for the skin, spars and ribs the 2D property Shell was chosen, which is translated in Nastran as a PSHELL card that defines the membrane, bending, transverse shear, and coupling properties of thin shell elements. The only geometric parameter is thickness, which will also be the optimization variable for Sol200.

For stiffeners 1D beam elements were chosen. For Nastran, this is the PBEAML element, which defines the properties of a beam element by cross-sectional dimensions, and in this case is L-shaped. For stringers 1D bar elements were chosen. For Nastran, this is the PBARL element, which defines the properties of a simple beam element (CBAR entry) by cross-sectional dimension, and in this case is Z-shaped.

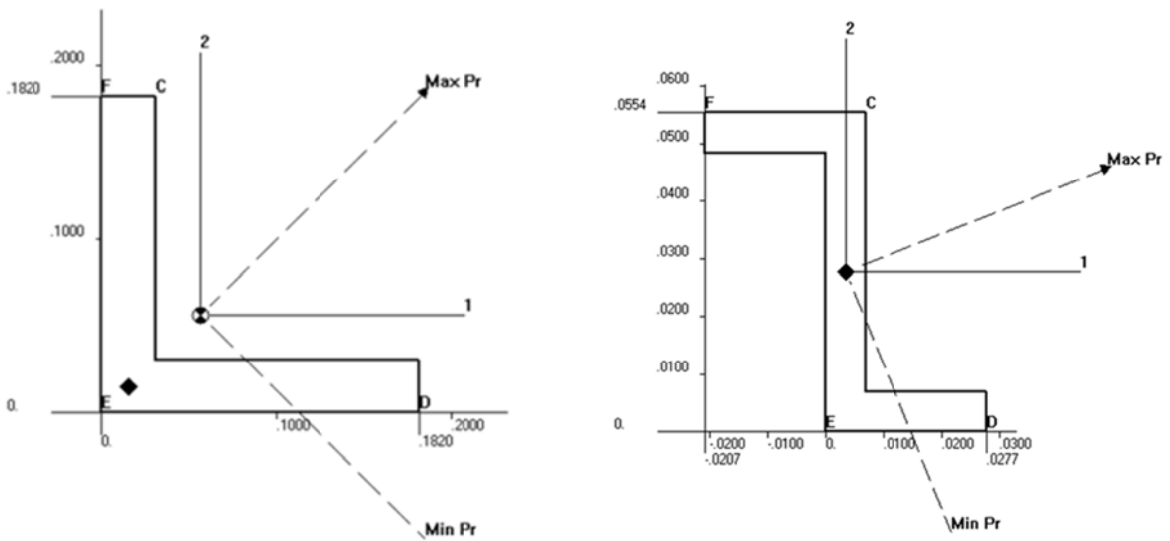


Figure 9 - L and Z shaped beam cross-section, primarily selected for stiffeners and stringers.

After studying the Sol200, it was revealed that changing the properties of a material is only possible with a linear relation of design variables and geometrical parameters, using DVPREL1 cards. This means that no complex geometry can be changed entirely, and for Z and L shaped beams, only one of its 4 parameters could be changed, still without complete accuracy - no inside parameters associations possible.

In this problem, it is considered that the stiffeners and stringers support only bending and shear moments, but not torsion. Since only the torsion analytical formula considers the difference between open and closed sections, and for the rest the cross section area that really is important, the simplest beam cross section was chosen for the continuation of the project, which is the circular one. Note that for complex beam cross section the optimization algorithm usually returns non accurate results when offset is defined.

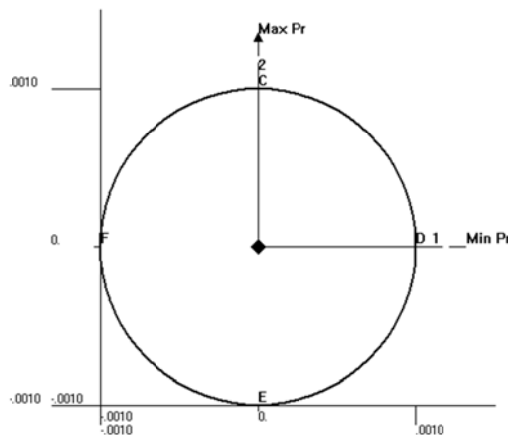


Figure 10 - Circular shaped beam cross-section used for stiffeners and stringers in final model.

The circular cross section has only the radius as input, so a single relation between a design variable and this radius defines all cross section properties. As a project definition, the stiffeners and stringers cross sectional areas are directly associated with the Wing-Box skin cross sectional area by the following way: the 2 upper corners stiffeners must have the same area as the 14 upper skin stringers; and the total area of upper stiffeners and upper stringers together must be the same as the upper Wing-Box skin area. The same correlations are applied for the lower skin and strips. Since Nastran doesn't accept DVPREL2 for this neither, a linear approximation was also used to associate skin and strips area relations, based on initial conditions provided by the reduced model, which change for each NACA profile.

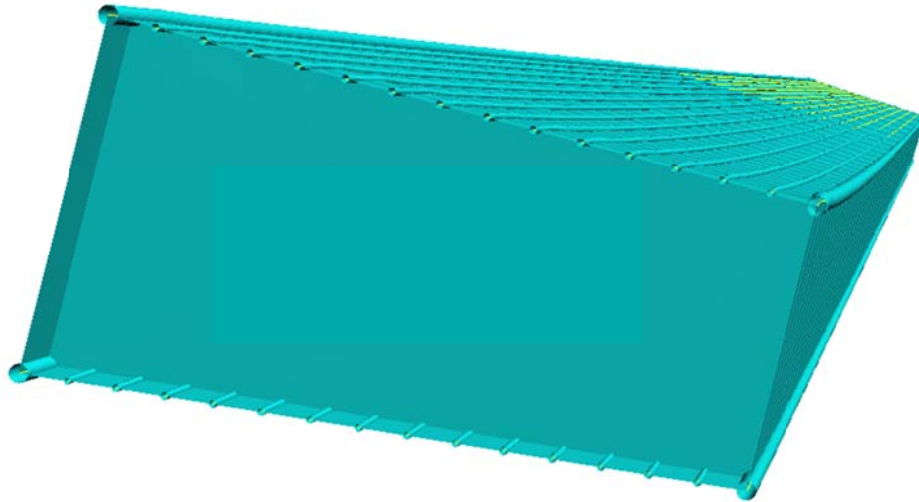


Figure 11 - Final wing-box configuration: skins, spars, stiffeners, stringers and ribs.

For Nastran, this is also a PBARL element, which defines the properties of a simple beam element (CBAR entry) by only one cross-sectional dimension - the radius - and in this case is a circular ROD cross section. The model studied also presents the correct beam offsets to respect the Wing-Box external geometric boundaries.

2.1.4 - Boundary Conditions

Since the studied Wing-Box comes from a cantilever wing, fixed on the fuselage, it's necessary to restrict all translational and rotational degrees of freedom in its root. In Nastran, this is done by a SPC1 card that defines a set of single-point constraints with $[T1 , T2 , T3] = [0 , 0 , 0]$ and $[R1 , R2 , R3] = [0 , 0 , 0]$ applied to the first rib surface.

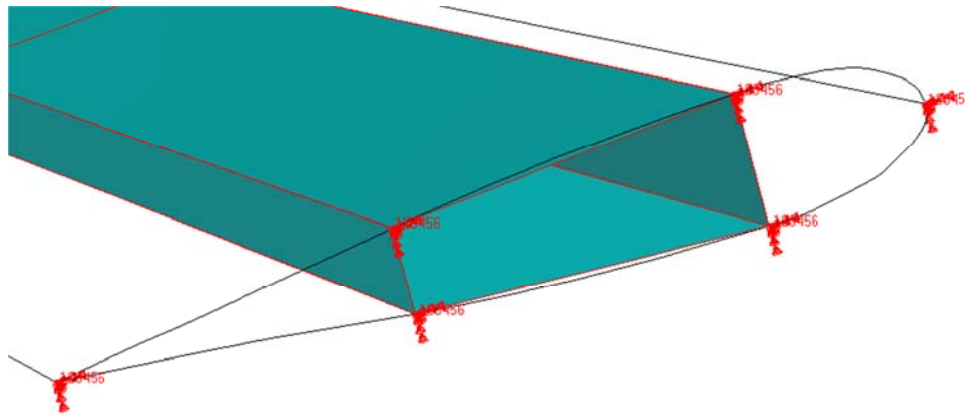


Figure 12 - Boundary conditions for cantilever wing: zero translation and rotation on first rib surface.

2.1.5 - Load Case

What concerns the load cases, for the preliminary design, just a few are relevant. In this study, the maneuver in altitude with MTOW and cruise speed will be the only load case considered. This is the most critical load case when designing the wing structure - other important cases are landing and crash. To go a little farther on the case adopted, it was decided to keep the MTOW but consider empty fuel wings because fuel alleviates the bending moment, so disregarding its presence provides an even more critical situation. Minimum thickness constraint will also be taken into account since industrial technologic limitations exists and must not be ignored.

In this study, cruise Mach is 0.79, cruise altitude is 12500 meters (41000 ft) and ISA atmospheric conditions are assumed. For maneuver in altitude, the critical load factor is considered to be $n_z = 2.5$ and the security factor is 1.5, so the extreme load factor according to FAR25.303 is $n_{zce} = 3.75$.

Another consideration is that the shear center was chosen to be the point of application of all forces and moments. In this way, all inertial forces were translated from the gravity center to the shear center, and the same for the aerodynamic forces on the aerodynamic center.

With this it is possible to resume all vertical forces to just one resultant, as well as for all bending moments and all torsion moments. Since drag is usually less than 1/17 of the aerodynamic lift, it was disregarded in this analysis, so no horizontal force is presented.

A deeper mathematical and physical approach is presented by Elodie Roux [8], so just the final equations are shown in this section. About the aerodynamic load, shear force, bending moment and torsion are taken into account. The lift was approximated to an elliptical distribution. The shear efforts and bending moment derive from this elliptical distribution, and torsion is consequence of the profile moment coefficient C_m . The non-dimensional approach is normalized by the half wingspan, where B is the wingspan, so:

$$Y = \frac{y}{B/2} \quad (13)$$

The total lift is also considered to be equal to the weight times the extreme load factor, so:

$$L = \frac{1}{2} \rho S V_a^2 C_z = n_{zc} \cdot MTOW \cdot g \quad (14)$$

The resultant forces, applied on the shear center of each Rib at Y position, are than a combination or aerodynamic and inertial forces:

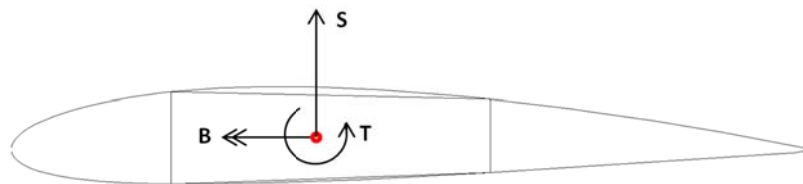


Figure 13 - Shear force, bending moment and torsion applied on shear center.

$$S(Y) = S_a(Y) + S_m(Y) \quad (15)$$

$$B(Y) = B_a(Y) + B_m(Y) \quad (16)$$

$$T(Y) = T_a(Y) + T_m(Y) \quad (17)$$

The following pictures better describe each term involved:

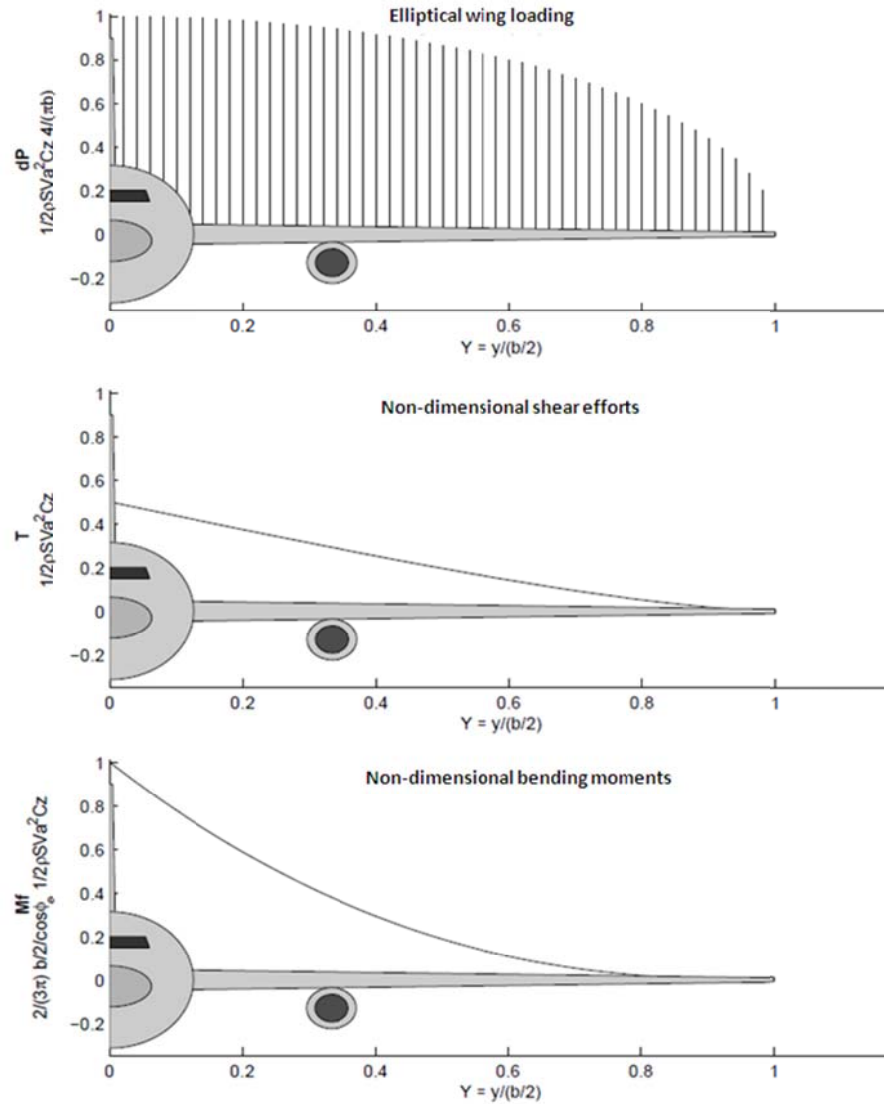


Figure 14 - Aerodynamic efforts at maneuver in altitude load case.

For the aerodynamic load, where ε is the profile maximum relative thickness, the final equations are:

$$S_a(Y) = L \cdot \frac{1}{2} \cdot \left(1 - \frac{2}{\pi} \cdot Y \cdot \sqrt{1 - Y^2} - \frac{2}{\pi} \cdot \sin^{-1} Y \right) \quad (18)$$

$$B_a(Y) = \left[\frac{2}{3} \cdot \frac{1}{\pi} \cdot \left(\frac{b}{2} \right) \right] \cdot L \cdot \left[(1 - Y^2)^{3/2} - \frac{3}{2} \cdot Y \cdot \left(\frac{2}{\pi} - Y \cdot \sqrt{1 - Y^2} - \sin^{-1} Y \right) \right] \quad (19)$$

$$T_a(Y) = \left(\frac{1}{2} \rho S V^2 C_{mprofil} \cdot \frac{C_r}{1 + \varepsilon} \right) \cdot \left[\frac{1}{3} \cdot (\varepsilon - 1)^2 (1 - Y^3) + (\varepsilon - 1)(1 - Y^2) + (1 - Y) \right] \quad (20)$$

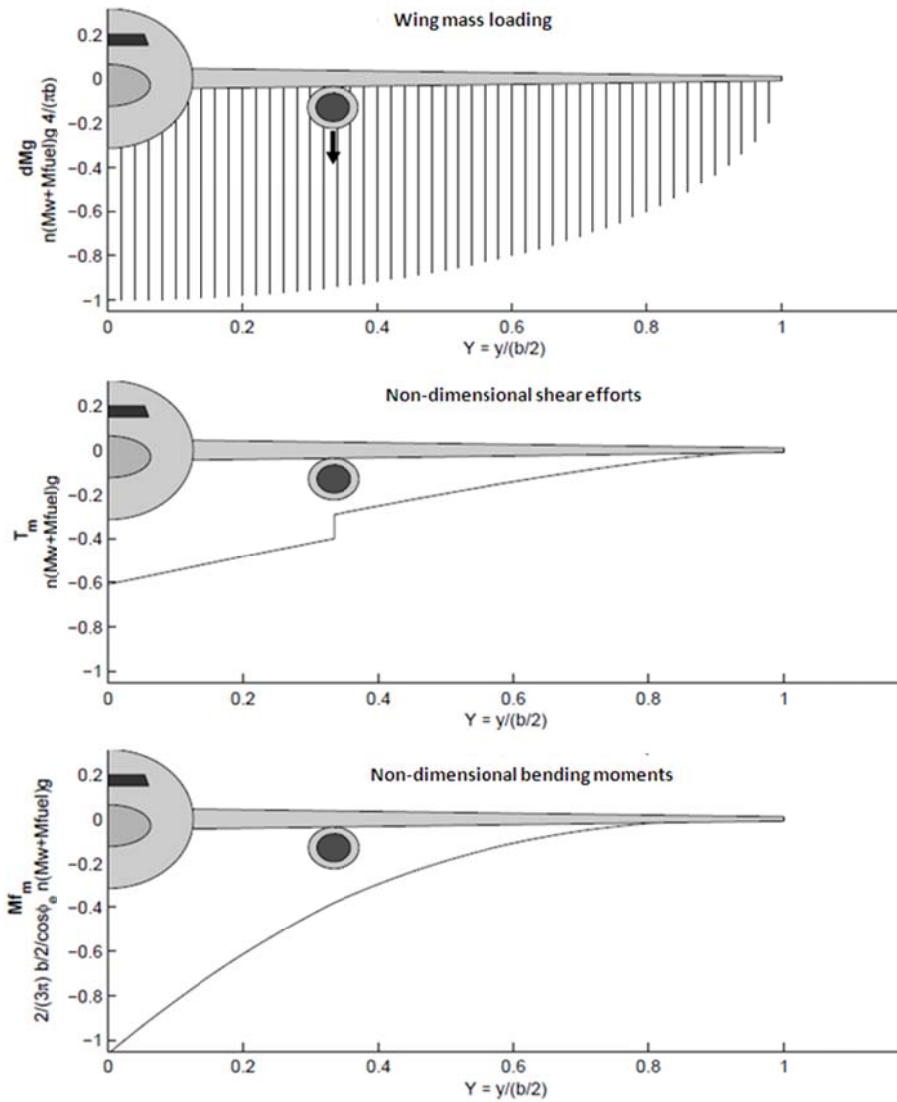


Figure 15 - Inertial efforts and due to the engine thrust at maneuver in altitude load case.

For the inertial and engine loads, two cases must be considered: before and after the engine, which is an element that changes totally the shear, bending and torsion efforts, since its mass and thrust are important and considered. The last term of each equation has two values where the first is for Y before the engine position Y_m , and the second for Y greater than Y_m . The final equations are:

$$S_m(Y) =$$

$$-n_{zce} \cdot (M_{wing} + M_{fuel}) \cdot g \cdot \frac{1}{2} \cdot \left(1 - \frac{2}{\pi} \cdot Y \cdot \sqrt{1 - Y^2} - \frac{2}{\pi} \sin^{-1} Y\right) - \left\{ \frac{n_{zce} \cdot M_{mot} \cdot g}{0} \right. \quad (21)$$

$$B_m(Y) = - \left[\frac{2}{3} \cdot \frac{1}{\pi} \cdot \left(\frac{b}{2}\right) \right] \cdot n_{zce} \cdot (M_{wing} + M_{fuel}) \cdot g \cdot \left[(1 - Y^2)^{3/2} - \frac{3}{2} \cdot Y \cdot \left(\frac{2}{\pi} - Y \cdot \sqrt{1 - Y^2} - \sin^{-1} Y\right) \right] - \left\{ \frac{3\pi \cdot M_{mot} \cdot (Y_m - Y)}{2 \cdot (M_{wing} + M_{fuel})} \right. \quad (22)$$

$$T_m(Y) = l_{CG_CS} \cdot C_r \cdot n_{zce} \cdot (M_{wing} + M_{fuel}) \cdot g \cdot \left[\frac{1}{2} \cdot \left(1 - \frac{2}{\pi} \cdot Y \cdot \sqrt{1 - Y^2} - \frac{2}{\pi} \sin^{-1} Y + \frac{4}{3\pi} \cdot (\varepsilon - 1)(1 - Y^2)^{3/2} \right) \right] + \left\{ \frac{d_M \cdot n_{zce} \cdot M_{mot} \cdot g - d_F \cdot F}{0} \right. \quad (23)$$

For aircrafts with wing mounted engines, the usual Y_m position is at 1/3 of half wing span. Since the studied wing has 29 ribs equally spaced, the 10th rib was chosen to fix the nacelle and support the engine. The engine's center of thrust is considered to be at $d_F = 1.30$ meters and $d_M = 3.43$ meters from the wing's shear center, and causes local torsion and bending due to its mass.

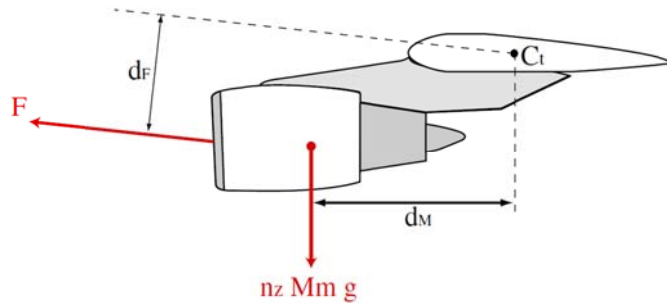


Figure 16 - Distances between thrust and weight points of application and the wing shear center.

Another important consideration is the fuel distribution along wingspan, which in this problem is also considered to be elliptical, although in the end zero fuel is admitted. l_{CG_CS} is the distance between the gravity center and the shear center. In this parametric modeling, for every single rib, a large group of parameters is changed due to scaling, translation and rotation. For these parameters, such as shear center and gravity center position, $C_{mprofil}$, initial wing mass, wing area / wing span, chord root, a direct interface with the reduced model [1] was created. Actually, since the numerical model is an optimization response for this model designed in Matlab environment and all parameters come from it, the first PCL code part is just variables declaration, all provided by it.

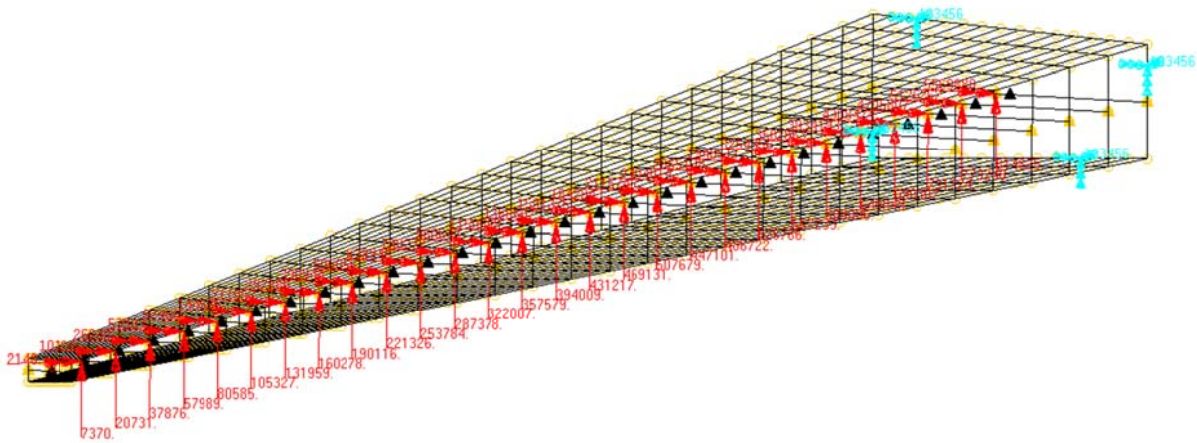


Figure 17 - Final load case applied to wing-box model in Patran.

In Nastran, forces are translated as FORCE cards that define a static concentrated force at a grid point by specifying a vector. The moments are translated as MOMENT cards that define a static concentrated moment at a grid point by specifying a scale factor and a vector that determines the direction. The loading case is grouped in a LOAD card that defines a static load as a linear combination of load sets defined via FORCE, MOMENT and other entries.

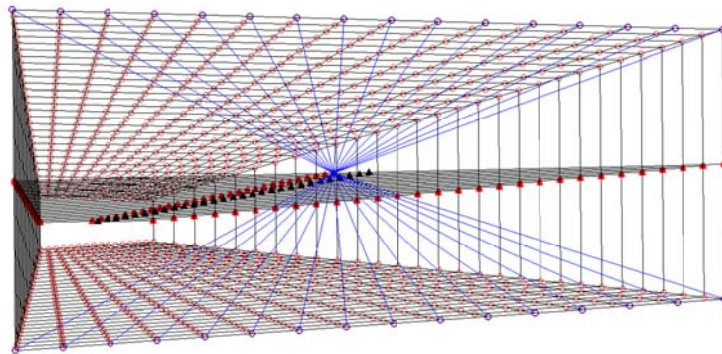


Figure 18 - Rigid Body Element REB2 used to distribute punctual efforts to entire wing-box section.

Since it was decided to apply the load distribution on the shear center of each rib, an unreal situation would be studied. To solve this problem, Nastran has an extremely useful tool called Rigid Body Element, or RBE2 card, which defines a rigid body with independent degrees-of-freedom that are specified at a single grid point and with dependent degrees-of-freedom that are specified at an arbitrary number of grid points. With this, it is possible to distribute the concentrated load to the entire model, and so have a more realistic solution.

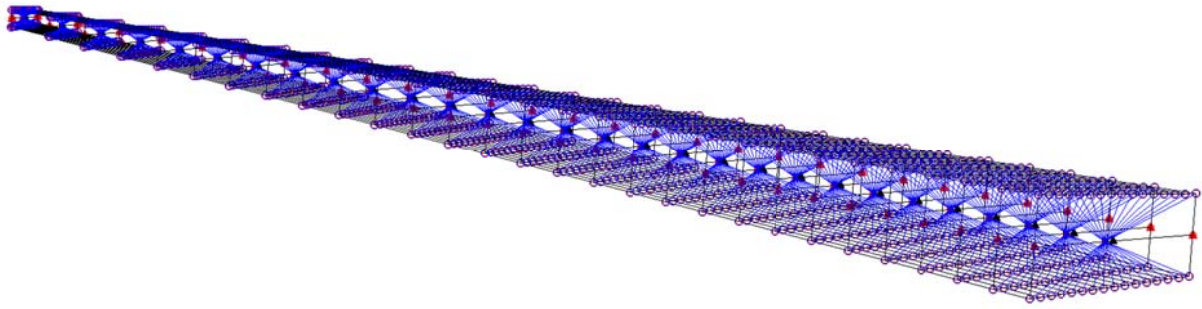


Figure 19 - Load distributed along wingspan with aid of REB2 elements.

2.1.6 - Meshing

For the meshing of the Wing-Box, a convergence study was made to have the lightest mesh. In optimization problems, increasing mesh refinement usually results in a much harder computational work, but a coarse mesh also prevents good results. A parametric mesh seed was implemented to give total control over the refinement so changing the number of elements is also a really simple work and doesn't take more than a few seconds.

When the optimization process in Sol200 started, it was found that optimizing a property is only possible if it has only one element. This means that creating a variable for thickness of a shell would only return descent results if the shell didn't have a refinement, since the analytical buckling formulation presumes constant flux, and n elements in one shell would give n different flux. In this way, each spar section has only one element, and each skin section has 15 elements - defined by the 2 stiffeners and 14 stringers.

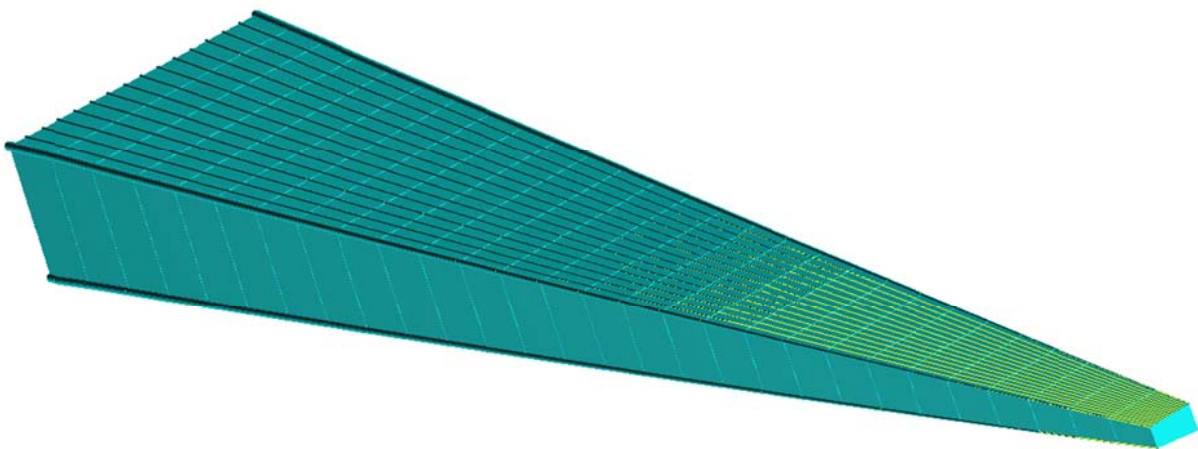


Figure 20 - Final wing-box mesh refinement.

For the 1D bar property, the Nastran translation for elements is CBAR. For the 2D shell, a Quad is the element shape, IsoMesh is the chosen mesher and Quad4 in the topology configuration. This means that all spars and skin elements are rectangles with the edge length controlled by the mesh seed. Nastran translates this by CQUAD4 elements that define an isoparametric membrane-bending or plane strain quadrilateral plate element. The ribs were meshed by paver that means irregular trapezoidal shapes.

All parameterization, even for the mesh, is extremely important since every studied wing has a completely different geometry (only dimensional parameters are kept constant). About geometry, 4 main input parameters change as well as hundreds of secondary parameters. About the properties, each section has 4 defined different skin thickness and 4 stringers and stiffeners geometrically correlated radius, and since there are 28 sections, at least 112 thickness are inputs that changes in every wing. With this amount of variables, a not all parameterized wing would cost and inestimable time spend in Patran, something absolutely not desirable.

2.2 - Nastran

Nastran is the world's most widely used Finite Element Analysis (FEA) solver. When it comes to simulating stress, dynamics, or vibration of real-world, complex systems, Nastran is still the best and most trusted software in the world. In this project, MSC Nastran 2007 is used for structural optimization. As presented before, the optimization process is based on equality and inequality constraints, side constraints and design variables, all associated by structural algorithms and processed by the optimizer.

The figure below shows how all these constraints and variables are used in developing the Design Model for Sensitivity and Optimization.

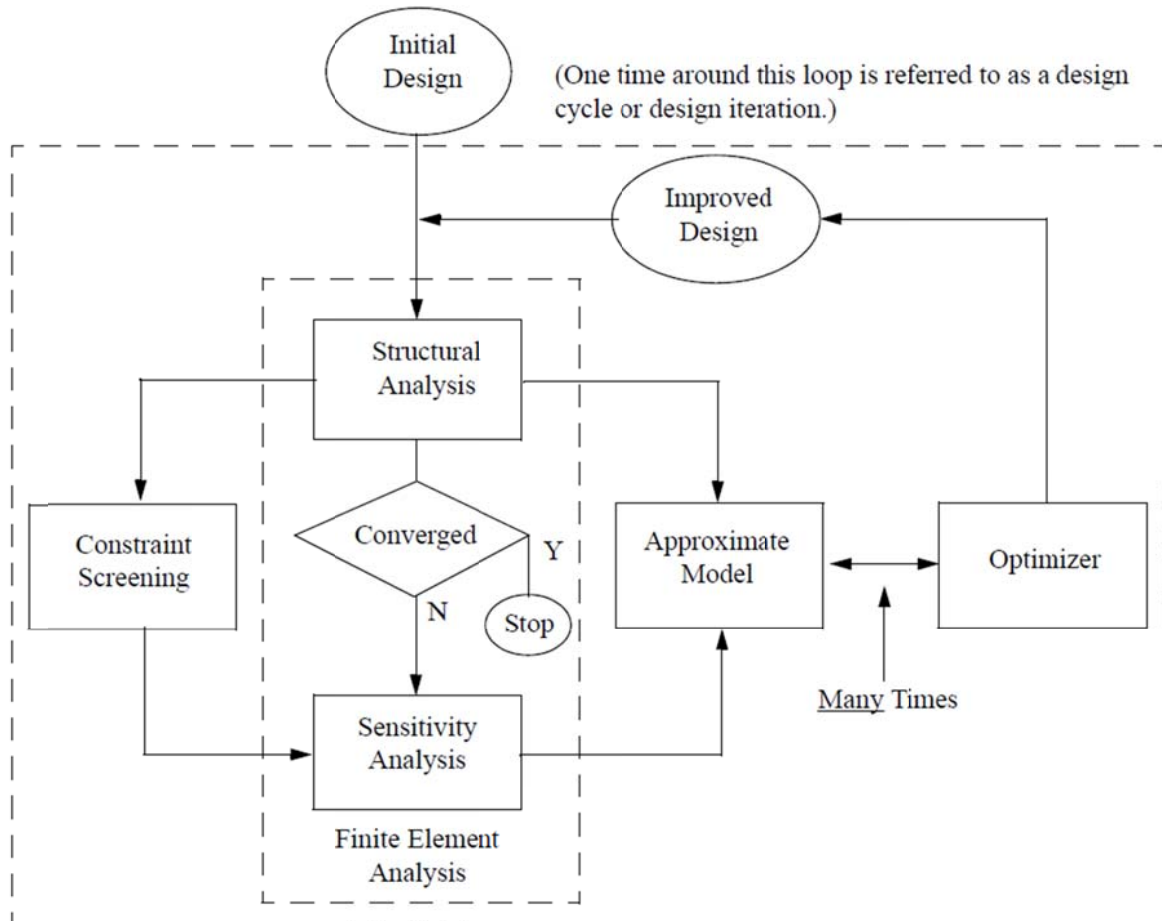


Figure 21 - MSC / MD Nastran implementation of Structural Optimization [3].

The initial design is a combination of the analysis model and the design model, which is a unique feature of the Design Sensitivity and Optimization capability. Structural analysis is the analysis function. However, for design sensitivity and optimization, it is frequently necessary to perform multiple types of analyses. This reflects the fact that the design responses can be created by a number of analysis types and it is necessary for the optimizer to synthesize these results when performing its redesign.

The concept of Constraint Screening is introduced in structural optimization and refers to the process that is used to identify those constraints that are likely to drive the redesign process. Accurate sensitivity analysis is the hallmark of Nastran implementation of design sensitivity and optimization. The individual analysis types each have their own techniques for performing sensitivity analysis and these are developed in Design Sensitivity Analysis.

For the optimizer, Nastran uses a variety of optimization algorithms from the MSCADS suite of algorithms as well as the IPOPT algorithm. The IPOPT algorithm is a special purpose optimization algorithm to address design tasks with a large number (> 3000 to 4000) of design variables and has its primary application to topology optimization tasks, but can be also applied to the conventional design tasks as well. Its access requires a Topology Optimization license. The IPOPT algorithm is open source code available from COIN-OR and maintained by IBM. It implements an interior point line search filter method. Structural optimization has also introduced the Approximate Model concept that involves the construction of high-quality approximations to the finite element results so that the number of full scale finite element analyses is kept to a minimum.

The Improved Design is the point at which the finite element model is updated based on the results from the optimizer so that a new finite element analysis can occur. Design Optimization is an iterative process and a key part of the implementation is therefore determining when to stop the iterations and set as converged. Tests for convergence discuss the many factors that enter into making this decision.

As for Discrete Variable Optimization, an underlying assumption of the Design Sensitivity and Optimization capability Nastran is that the variations in the design variables are continuous and that therefore the responses and their sensitivities are also continuous. Practical engineering considerations frequently dictate that values of the designed properties be chosen from a discrete set.

Finally, the Topology Optimization is a special version of design optimization that finds an optimal distribution of material, given package space, loads and boundary conditions. Basically, it makes a design variable out of each finite element that can vary from 0 (remove) to 1 (keep) and the algorithm strives to force real design variables to one of these limits. In this project Topology optimization will not be approached.

2.2.1 - Sol200

The Sol200 doesn't have a GUI interface in Patran, since it's designed to support a really large number of variables (up to 12 millions) and constraints. It also has a specific language that respects some rules and presents Nastran unique cards. To write in Sol200, a secondary program is required, since the code usually exceeds thousands of lines. A Python macro may be useful, but usually Matlab or Excel is used. In this project, Excel aided generating the .bdf file, which has more than 11.000 lines. A Nastran bdf file is basically structured the following way:

```

NASTRAN SOL200

..... }
..... } EXECUTIVE CONTROL DECK
..... }
..... }

CEND

..... }
..... } CASE CONTROL DECK
..... }
..... }

BEGIN BULK

..... }
..... } BULK DATA
..... }

ENDDATA

```

The Executive Control Deck indicates what type of solution.

- TIME: maximum execution time allowed;
- SOL 200: design sensitivity and optimization solution;
- CEND: indicates the end of the Executive Control.

The Case Control Deck is responsible for controlling the execution of tasks.

- ANALYSIS: the type of analysis (STATICS, DFREQ, BULK, MODES, etc.);
- TITLE: the algorithm title is given;
- MAXLINES: define the maximum number of output lines;
- DESOBJ: select a design variable as the objective function;
- DESGLB: select the constraints to be respected;
- PARAM, X: control the output for post-processing;
- BEGIN BULK: indicates the end of the Case Control.

The Bulk Data is where all elements, variables, constraints, materials, properties, and any information associated to the model and its solution are declared. The model is obtained by Sol101 translated by Patran to Nastran in the form of a bdf file. From this file, only the grid, elements, materials, properties, loadings and boundary conditions are imported to Sol200. After declaring the model, the unique Sol200 design variables and constraints are declared, and finally the design optimization parameters in the form of a DOPTPRM card. For this specific study, the entire process is represented by the following diagram.

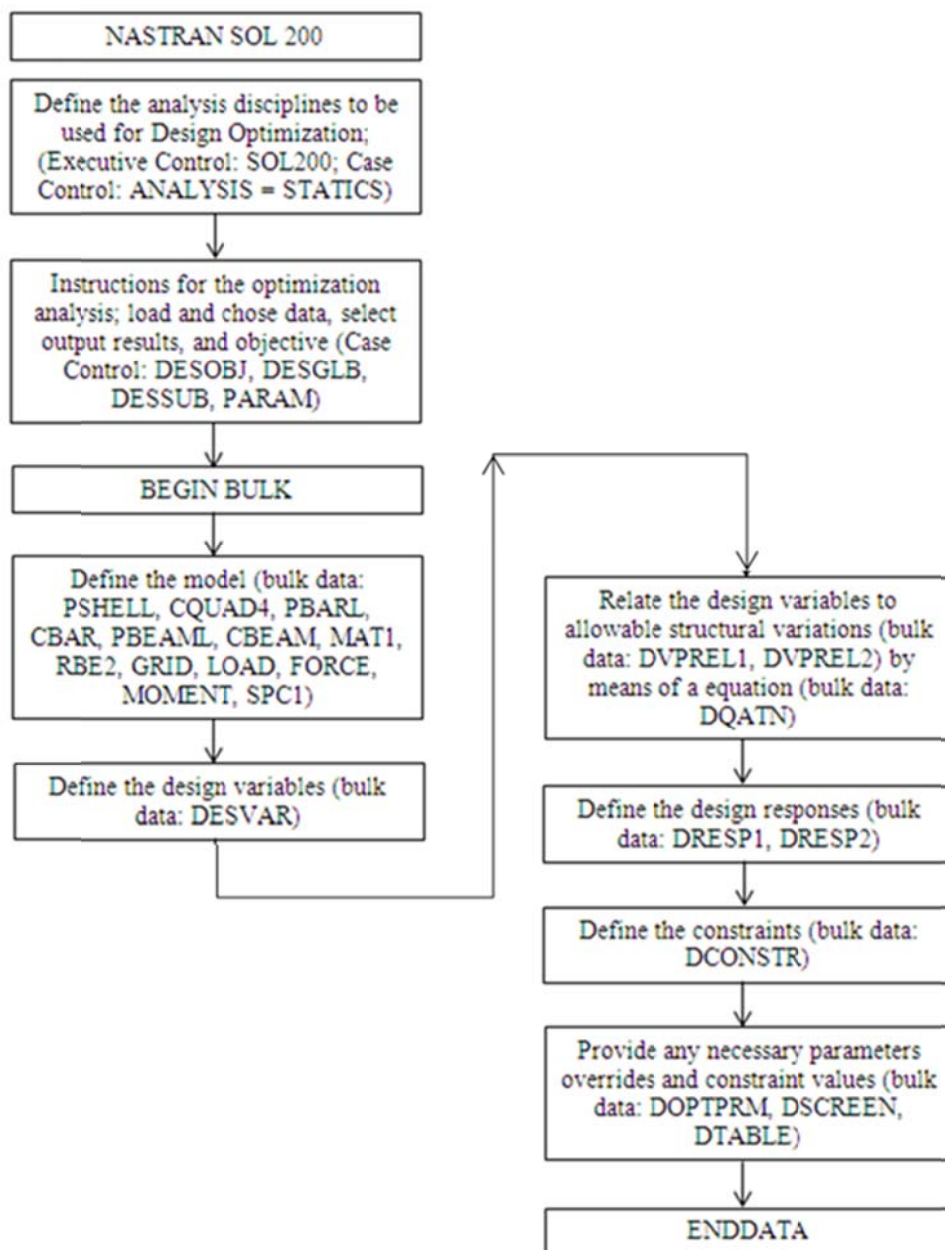


Figure 22 - MSC / MD Nastran Sol200 Design Modeling Process.

2.2.2 - Analysis

The analysis proposed is based on a static load, and the main objective is to optimize the entire Wing-Box according to buckling and maximum shear stress criteria, strain criterion and maximum wing tip displacement. With a cantilever wing, given the load case, it's possible to calculate the minimum thickness for each part respecting the structural constraints. A global optimization will find the best thickness combination that will reduce the Wing-Box weight to a global minimum.

2.2.3 - Design Variables

The chosen independent design variables are the section shell thickness of each structure, and this means 4 structures (upper and lower skins, front and rear spars) in each of the 28 sections, so 112 design variable. In Nastran, this is programmed by a DESVAR card, which defines the design variables to be used in design sensitivity and optimization. Design sensitivity analysis computes the rates of change of design responses with respect to changes in the design variables. In design optimization, the set of design variables are the quantities modified by the optimizer in the search for an improved design. The optional DESVAR Case Control command can be used to specify the set of DESVAR Bulk Data entries that are to be used in the design task.

The upper WB corner stiffeners and upper WB skin stringers also received a design variable each, as well as the lower ones. This means 4 more variables for each section, but these 112 variables are dependent of the 56 WB skin thickness variables. This is possible through DLINK cards that relate one design variable to one or more other design variables by linear relation. The linear relation, in this case, is based on the area distribution between WB skin, stiffeners and stringers, as mentioned before.

The design response that will be globally optimized is the total weight, and Nastran has already a specific entry in DRESP1 card for this action called WEIGHT. The total of design variables is so 224.

2.2.4 - Criteria and Constraints

The Upper Skin presents compression stress and shear stress as critical stresses. The criteria used are than the material yield and local buckling. The equation in this case is a combination of compression and bucking criteria:

$$\frac{\sigma_{comp}}{(\sigma_{comp})_{cr}} + \left(\frac{\tau_{xy}}{(\tau_{xy})_{cr}} \right)^2 \leq 1 \quad (24)$$

Where:

$$(\sigma_{comp})_{cr} = \frac{\eta_c K_c \pi^2 E}{12(1-\nu^2)} \left(\frac{t}{b} \right)^2 \quad (25)$$

$$(\tau_{xy})_{cr} = \frac{\eta_s K_s \pi^2 E}{12(1-\nu^2)} \left(\frac{t_s}{b} \right)^2 \quad (26)$$

About these equations, $\eta_c = 1.0$ and $\eta_s = 1.0$; $K_c = 4.0$ $K_s = 5.4$ and $t_s = 0.5t$. For the upper skin Al 7150 T7751 is used, so $E = 71.016$ GPa and $\nu = 0.3$. Nastran provides the stresses in both skin boundary surfaces, so in this study an average was taken to better results, although it's considered to be a thin shell.

The parameter b is the distance between 2 consecutive stringers that define the boundaries for local buckling. The Wing-Box skin is divided by 14 stringers and 2 stiffeners, so 15 segments compose the Wing-Box chord. In this way, b is considered to be 1/15 of 40% of the local wing chord, approximately.

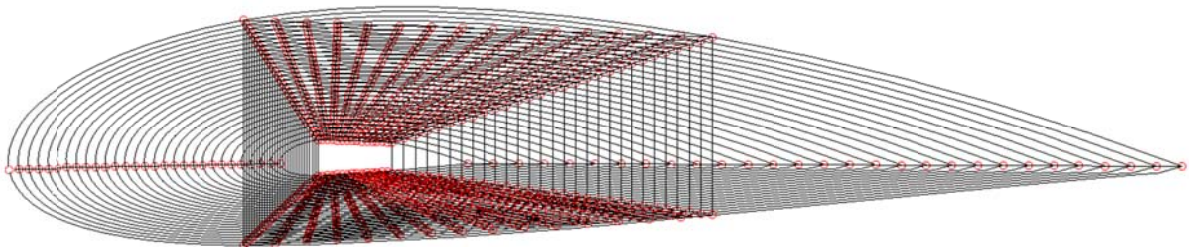


Figure 23 - Wing-Box configuration inside the wing using NACA 4420 profile.

The Lower Skin presents tension stress and shear stress as critical stresses. The criterion used is than the maximum distortion energy yield, so the Von Misses Criterion was adopted. The equation is so:

$$\frac{f_{ty}}{\sigma_{vm}} \geq 1 \quad (27)$$

For the Al 2024 T351 Bare, used in the lower skin, $f_{ty} = 290.0$ MPa, and the Von Misses stress is given directly by Nastran, so it's not necessary to calculate it by analytical formula. The Von Misses used is also an average of both provided by Nastran.

The Front and Rear Spars presents the same behavior, so the exactly same approach was adopted for both structures. The critical stress is the shear stress, and the shear criterion was adopted. The equation is:

$$\frac{(\tau_{xy})_{cr}}{\tau_{xy}} \geq 1 \quad (28)$$

Where:

$$(\tau_{xy})_{cr} = \frac{\eta_s K_s \pi^2 E}{12(1-\nu^2)} \left(\frac{t_s}{b}\right)^2 \quad (29)$$

In this case, $\eta_s = 1.0$ and $K_s = 5.4$. For the upper skin Al 2024 T351 Bare is used, so $E = 73.774$ GPa and $\nu = 0.3$. Nastran provides the shear stresses in both skin boundary surfaces, so an average was again taken.

Another criteria adopted is the maximum wingtip vertical displacement that shall not pass 1,7 meters. In fact, for Airbus A320 wing, the destructive test shows a maximum deformation of 2,5 meters, and considering a safety marge of 50%, the adopted value is acceptable. This is a criterion also used in aeronautical industry for psychological aspect, since a huge wing deformation may cause panic between passengers.

$$d_{y,tip} \leq 1,7 \text{ meter} \quad (30)$$

The strain criterion is also taken into account. For modern aluminum alloys, the limit is around 4 micro deformations, so:

$$-4 \cdot 10^{-3} \leq \varepsilon \leq 4 \cdot 10^{-3} \quad (31)$$

In Nastran Sol200 language, a DTABLE card defines a table of constants to be used in conjunction with DEQATN equations. A DRESP1 card defines direct, or first-level, analysis responses to be used in design sensitivity and optimization. The responses identified here are those which are directly available from the analysis results as opposed to second-level responses which are defined using DRESP2 and DEQATN entries. This means all stress, strain, displacement or any output given directly from Nastran structural calculus will be given in a form of DRESP1.

The DRESP2 card defines equation responses that are used in the design process, either as constraints or as an objective. It's in this type of card that the criteria are inserted, with aid of a DQATN card that defines equations for use in synthetic relations. These equations can be used to define either second-level responses or second-level design variable-to-property relations. The constraints limits are imposed by DCONSTR cards that places limits on a design response. When selected in Case Control by either DESGLB or DESSUB, the DCONSTR sets define the design constraints. Finally, the relation between an analysis model property and design variables is made by DVPREL1 cards.

2.2.5 - Design Optimization Parameters

There are numerous parameters that control various aspects of the optimization process itself. While all of these parameters have defaults (the DOPTPRM entry is optional), the defaults may be changed using the DOPTPRM card entry which overrides default values of parameters used in design optimization.

There are three types of approximation methods to choose from in Sol200: direct linearization, mixed method, and convex linearization. The mixed method is the default but in this study, the direct linearization (APRCOD = 1) will be used. It's based on the simple first-order Taylor series expansion directly in terms of the design variables. The method is often useful for dynamic response optimization, shape optimization, and optimization tasks that use basis vector formulations.

The optimization process is iterative since the optimizer obtains data about the design space from approximations. The approximate model, constructed based on a detailed finite element analysis, is used by the optimizer to find an approximate optimum. This design is resubmitted for another finite element analysis followed by another approximate optimization. This process is repeated until convergence with respect to these overall design cycles is reached or until the maximum specified number of design cycles (DESMAX) is reached. In this problem DESMAX was adjusted to 50.

As the optimizer modifies the design variables, the structure's properties and/or shape will vary depending on the design model description. Move limits need to be placed on the approximate sub problem for efficiency reasons and these move limits are imposed with respect to analysis model properties as well as design variables. They can be changed from their defaults by modifying DELX for design variables, which defines rational change allowed in each design variable during any optimization cycle, and was set to 0,5.

The parameter CONV1 is used to test for overall design cycle convergence. It is the Relative criterion to detect convergence. If the relative change in objective between two optimization cycles is less than CONV1, then optimization is terminated. This parameter is used in connection with tests for both hard and soft convergence. Tests for Convergence describe the types of convergence testing as well as the convergence decision logic. Soft convergence compares the design variables and design properties output from the approximated model optimization with these same values at the beginning of the design cycle. Hard convergence testing compares the analysis results of current design cycle with those of the previous cycle. This test is a more conclusive test of convergence since it is based on hard evidence. Hard convergence will always terminate the design cycle process.

The DELOBJ defines maximum relative change in objective between ITRMOP consecutive iterations to indicate convergence at optimizer level, and was set to 1.0E-3. The ITRMOP defines the number of consecutive iterations for which convergence criteria must be satisfied to indicate convergence at the optimizer level, and was set to 3.

The relative change in objective attempted on the first optimization iteration is controlled by DOBJ1. Used to estimate initial move in one-dimensional search, it is adapted as the optimization progresses, and is set to 0,1. The minimum move limit imposed by DPMIN is 0,01, and the minimum design variable move limit imposed by DXMIN is 0.05. The constraint normalization factor GSCAL used is 1.0E-3, and finally the optimization METHOD adopted is the Modified Method of Feasible Directions for both MSCADS and DOT.

3.1 - Non-Optimized WB (Part I)

In this first part, the NACA 2420 Wing-Box was directly constructed from the inputs provided by the Reduced Model, which means without any optimization. The spars and skins thickness are based on an analytical model that considers only the stress criteria and all calculus were made on Matlab environment. The 112 inputs were inserted in Patran PCL code without any processing, and the model analyzed by Nastran Sol101.

The results show a Wing-Box of 2091,83 Kg (total mass, including skin, spars, ribs and strips). The maximum vertical wing tip displacement is 2,008 meters, which is a huge displacement for a semi-wing of only 19 meters, and the shear stress in shell elements arrives up to 2,5 GPa that overpasses the resistance of any metallic material possibly used in a wing. The following pictures show the bending, total displacement and stress tensor on the deformed Wing-Box (real scaling).

The first and last pictures show that stress is not well distributed along span, and it's visible that the wing tip is not supporting any efforts (painted in white). The Total Displacement picture gives the real wing tip displacement dimension, which might not tolerated by aerodynamics since lift vector starts to have an important horizontal component. Note that these pictures are presented only for quantitative analysis and comparison with the following analysis, and the Upper Skin and Rear Spar are the visible parts.

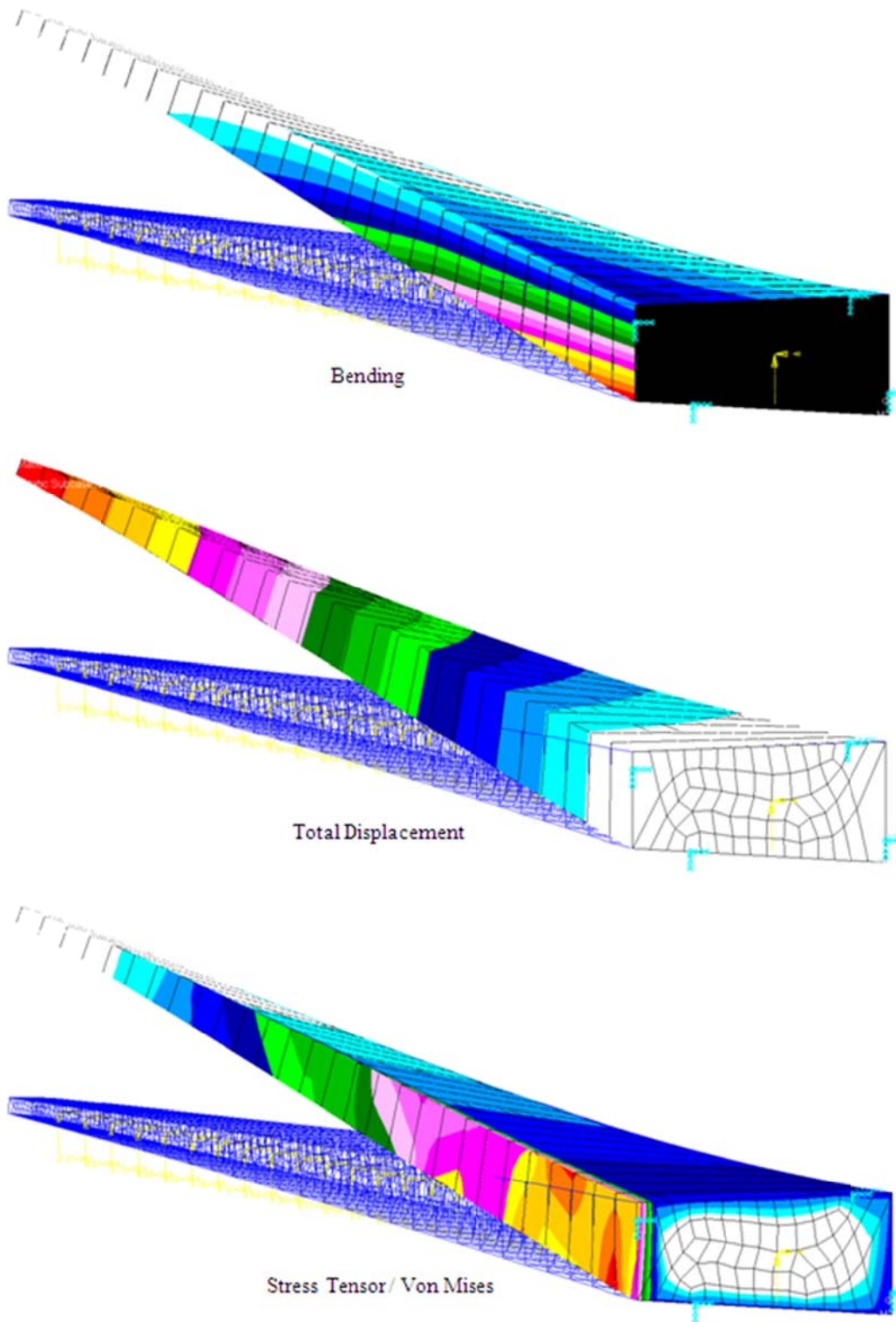


Figure 25 - Bending, Total Displacement and Stress Tensor for NACA 2420 profile WB, Static Analysis without optimization.

3.2 - WB optimized by Stress Criteria only (Part II)

In this second part, the Wing-Box was optimized by Sol200 based on only stress criteria, as presented before. This approach is a response for the Reduced Model [1] that uses these results for its Surrogate Model. The 112 thickness variables were redefined to give the minimum global weight respecting all constraints. The other 112 stringers and stiffeners variables were also redefined accordingly to the area relations that define its dependency to the thickness variables. For the NACA 2420, optimization took 18 cycles to converge, and the mass reduction can be seen on the picture below.

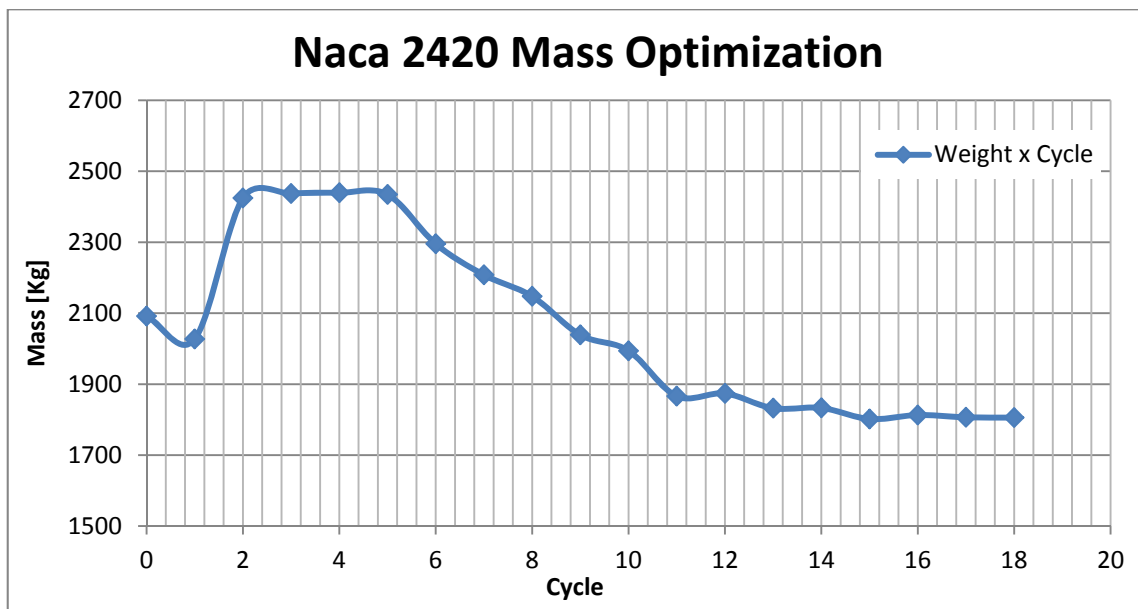


Figure 26 - Mass optimization for NACA 4420 profile WB, Static Analysis optimized by Sol200 with stress criterion only, 18 cycles total.

After the 18 cycles, the results converge to a weight of 1805,88 Kg, that is a total reduction of 13,7% or 286 Kg on each semi-wing, a considerable amount in terms of aeronautics. Just to have an idea, the total weight reduction of 572 Kg is more than the total crew weight specified by FAR Part 25, for this class of transport aircraft (A320 and Boeing 737-800). The following table presents the mass in each cycle. The initial mass was 2091,83 Kg.

Table 1 - Mass optimization process in Sol200 for the 18 cycles with stress criterion only for NACA 2420 profile WB, in Static Analysis. Initial Weight 2091.83 Kg.

Cycle	1	2	3	4	5
Total Mass [Kg]	2027,34	2424,46	2437,31	2439,26	2434,34
Cycle	6	7	8	9	10
Total Mass [Kg]	2295,56	2207,87	2147,50	2038,73	1994,06
Cycle	11	12	13	14	15
Total Mass [Kg]	1866,19	1873,71	1832,16	1833,08	1801,77
Cycle	16	17	18	-	-
Total Mass [Kg]	1813,02	1806,55	1805,88	-	-

Now the optimization results will be presented for each of the four aimed parts: Front Spar, Rear Spar, Upper WB Skin and Lower WB Skin. Each part presents 28 sections (series on the legend), and for each one the thickness optimization for each section will be presented (for the 18 cycles) and also the final thickness along span, before and after optimization.

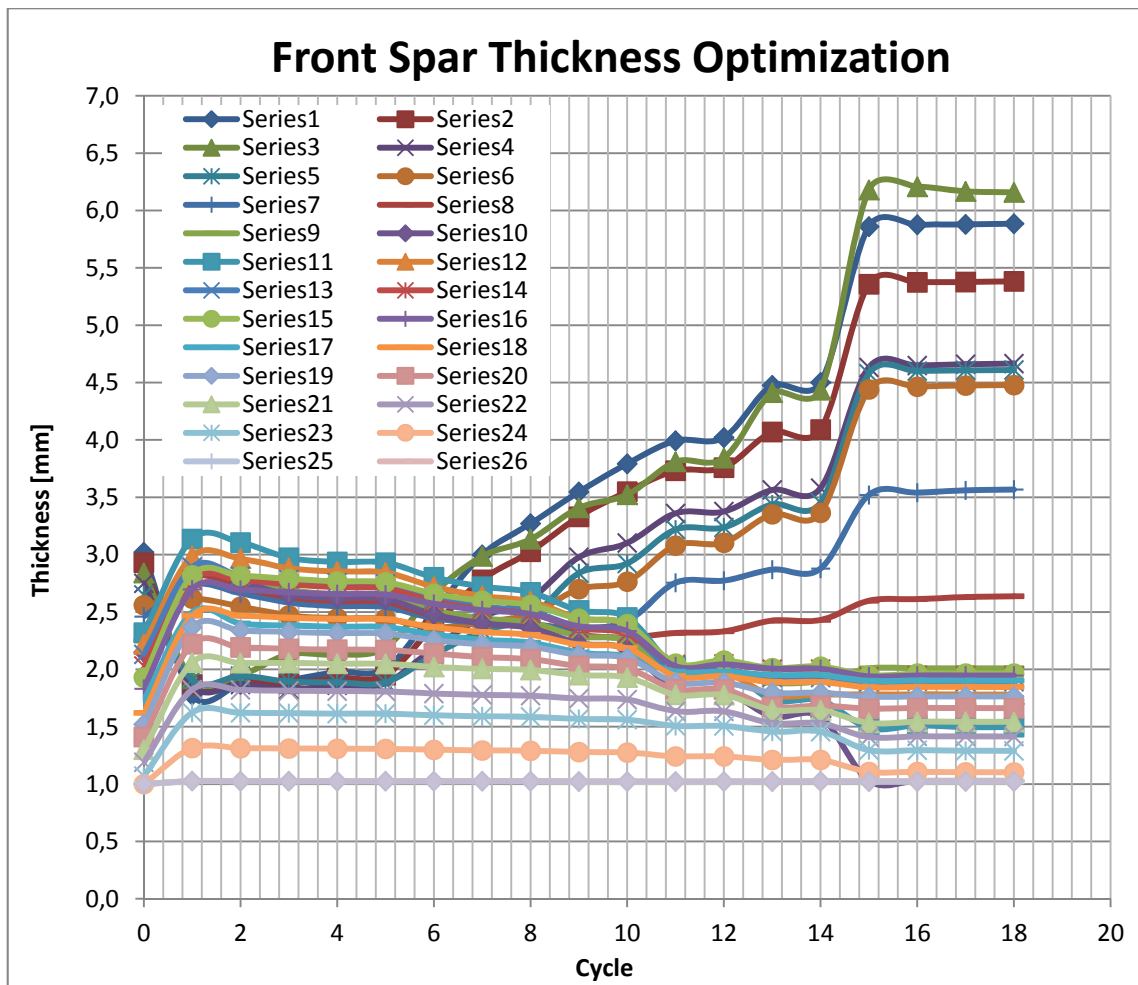


Figure 27 - Front Spar thickness optimization for the 28 sections in Sol200 with stress criterion only for NACA 2420 profile WB, in Static Analysis, 18 cycles total.

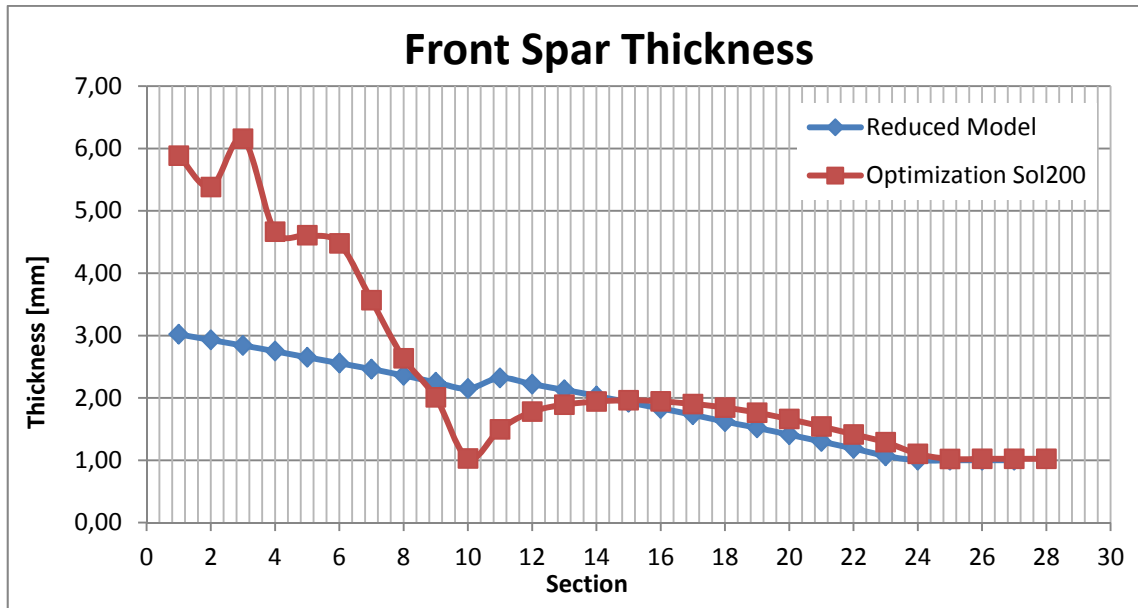


Figure 28 - Front Spar thickness before and after optimization in Sol200 for the 28 sections with stress criterion only for NACA 2420 profile WB, in Static Analysis.

For the front spar, thickness decreases up to the 10th section, just before the engine. From the 11th section to the 17th it increases again and then decreases to the minimum thickness. Globally it's visible that the optimization increased the thickness distribution before the 10th rib, showing that the engine affects greatly the front spar, being decisive when designing this part of the Wing-Box.

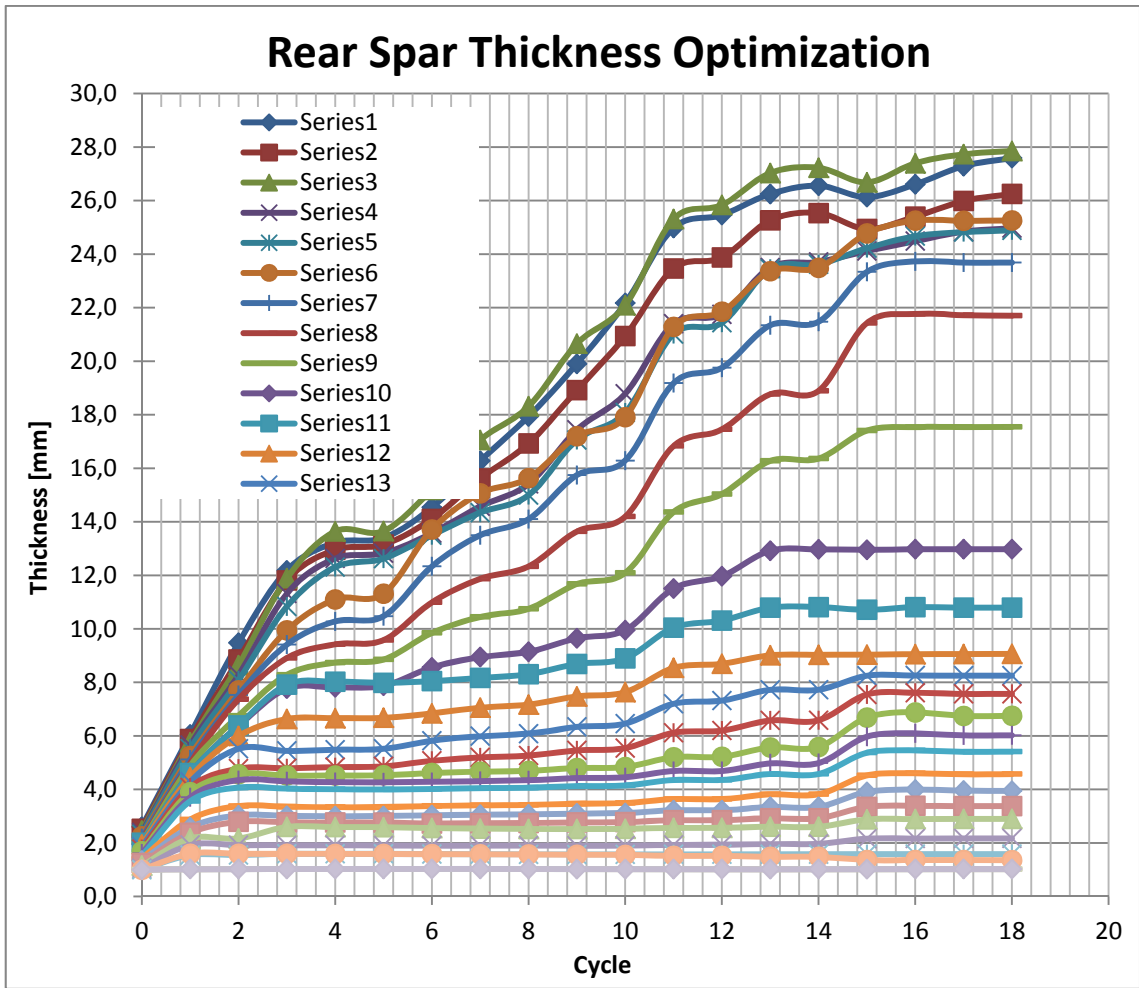


Figure 29 - Rear Spar thickness optimization for the 28 sections in Sol200 with stress criterion only for NACA 2420 profile WB, in Static Analysis, 18 cycles total.

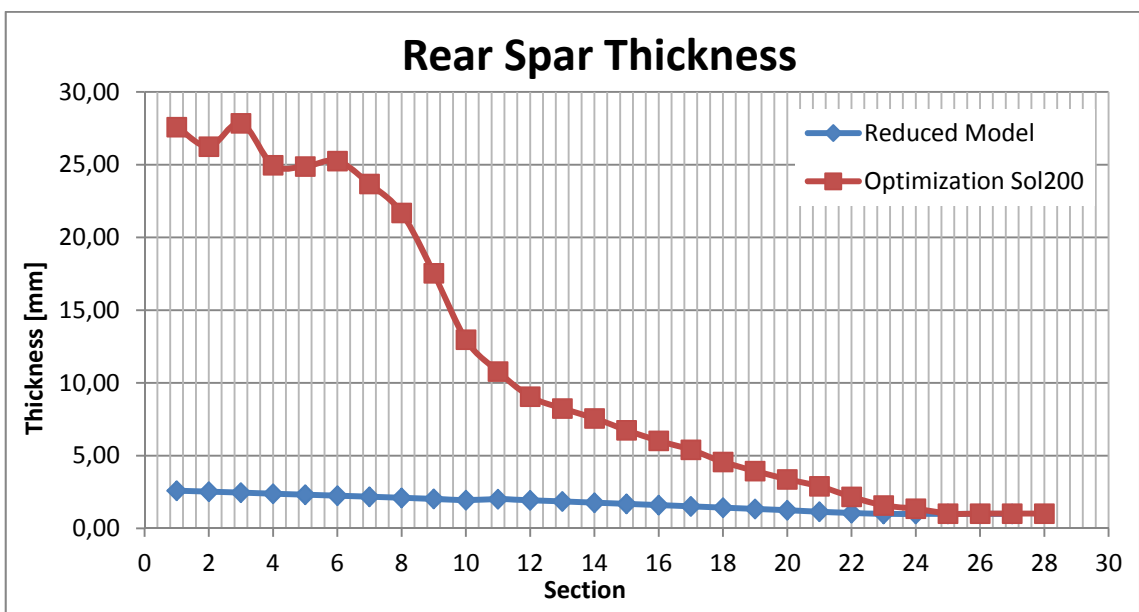


Figure 30 - Rear Spar thickness before and after optimization in Sol200 for the 28 sections with stress criterion only for NACA 2420 profile WB, in Static Analysis.

For the rear spar, on other hand, optimization increases strongly the thickness of every section up to the 25th. The first 4 sections has even an increase of thickness by the order of 10 times, showing that in terms of a globally optimized structure, the rear spar is not well designed by the analytical model. It's important to remember that the numerical solution considers the interaction between all elements of the model, and so the response may be extremely different than expected. After optimization, the rear spar is totally different than the initial structure, but still the engine influences the design process, since greater thickness increment can be found before the 10th rib.

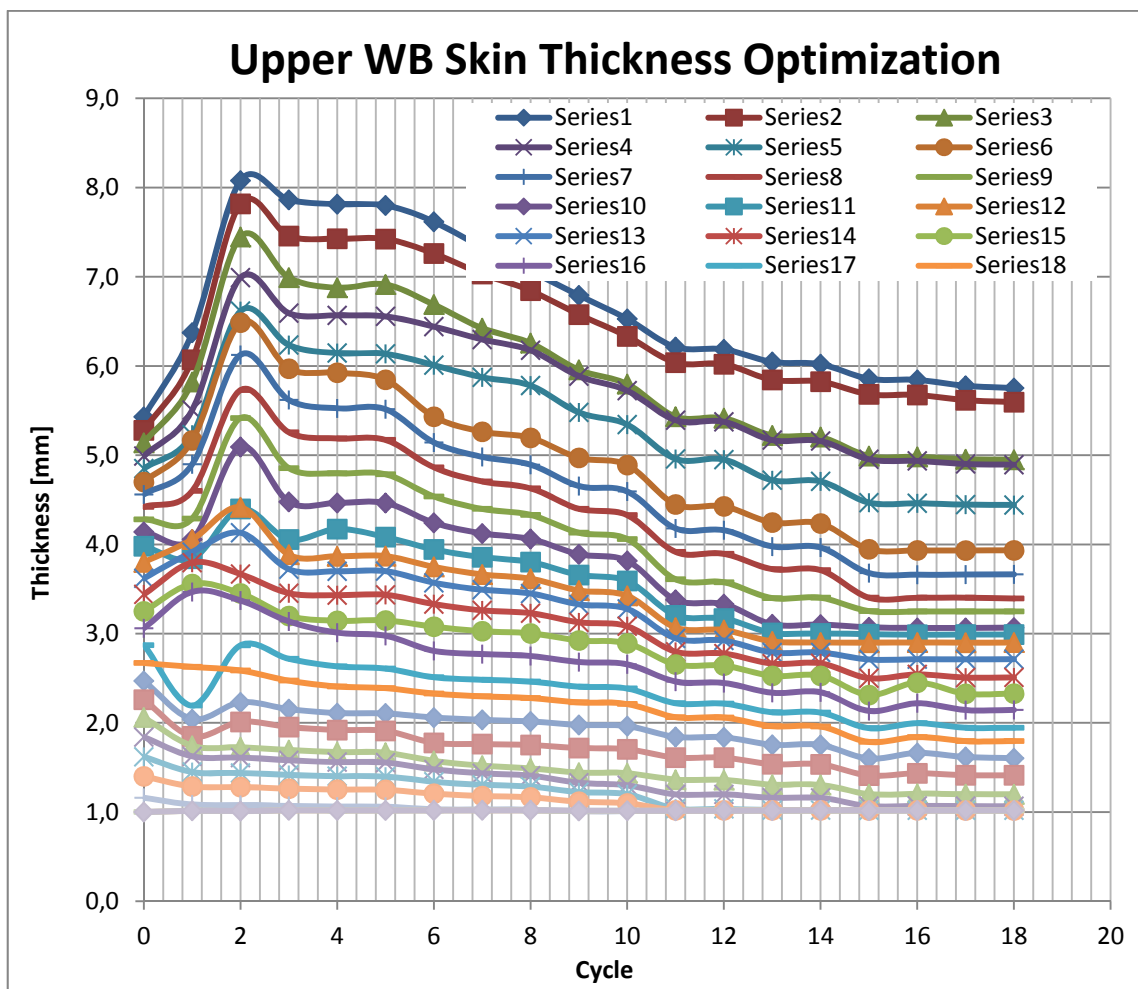


Figure 31 - Upper WB Skin thickness optimization for the 28 sections in Sol200 with stress criterion only for NACA 2420 profile WB, in Static Analysis, 18 cycles total.

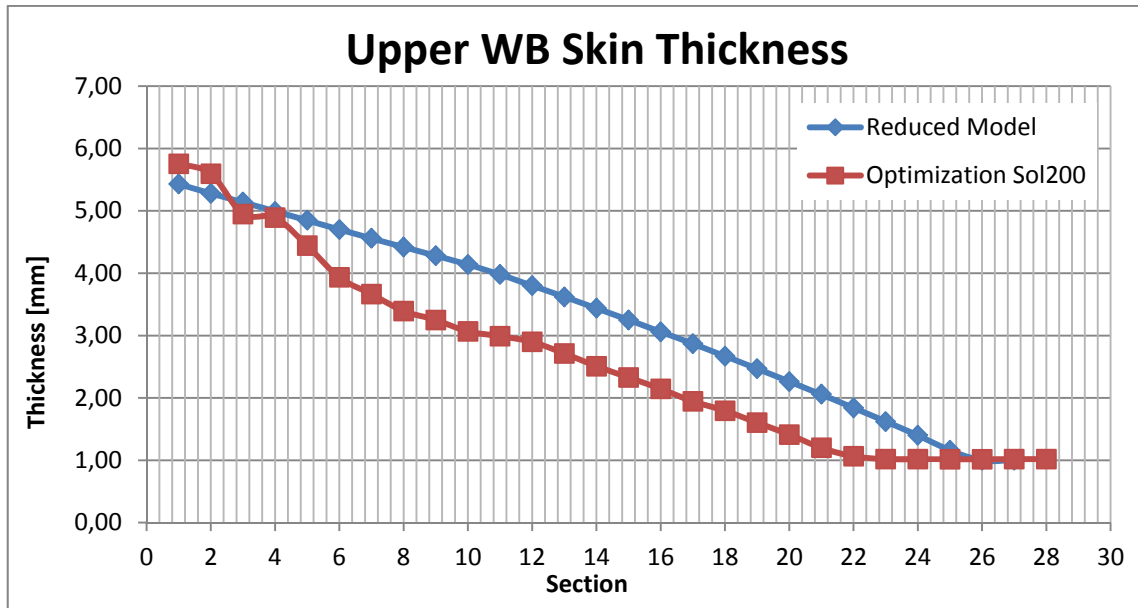


Figure 32 - Upper WB Skin thickness before and after optimization in Sol200 for the 28 sections with stress criterion only for NACA 2420 profile WB, in Static Analysis.

The behavior of the upper WB skin is completely different from the spars. In fact the optimization doesn't change much the section thickness, and the final results follow not by far the initial design. But in this case, the overall thickness decreases, and the engine influence is not visible. Almost 30% of the upper WB skin rests with the minimum 1,00mm thickness.

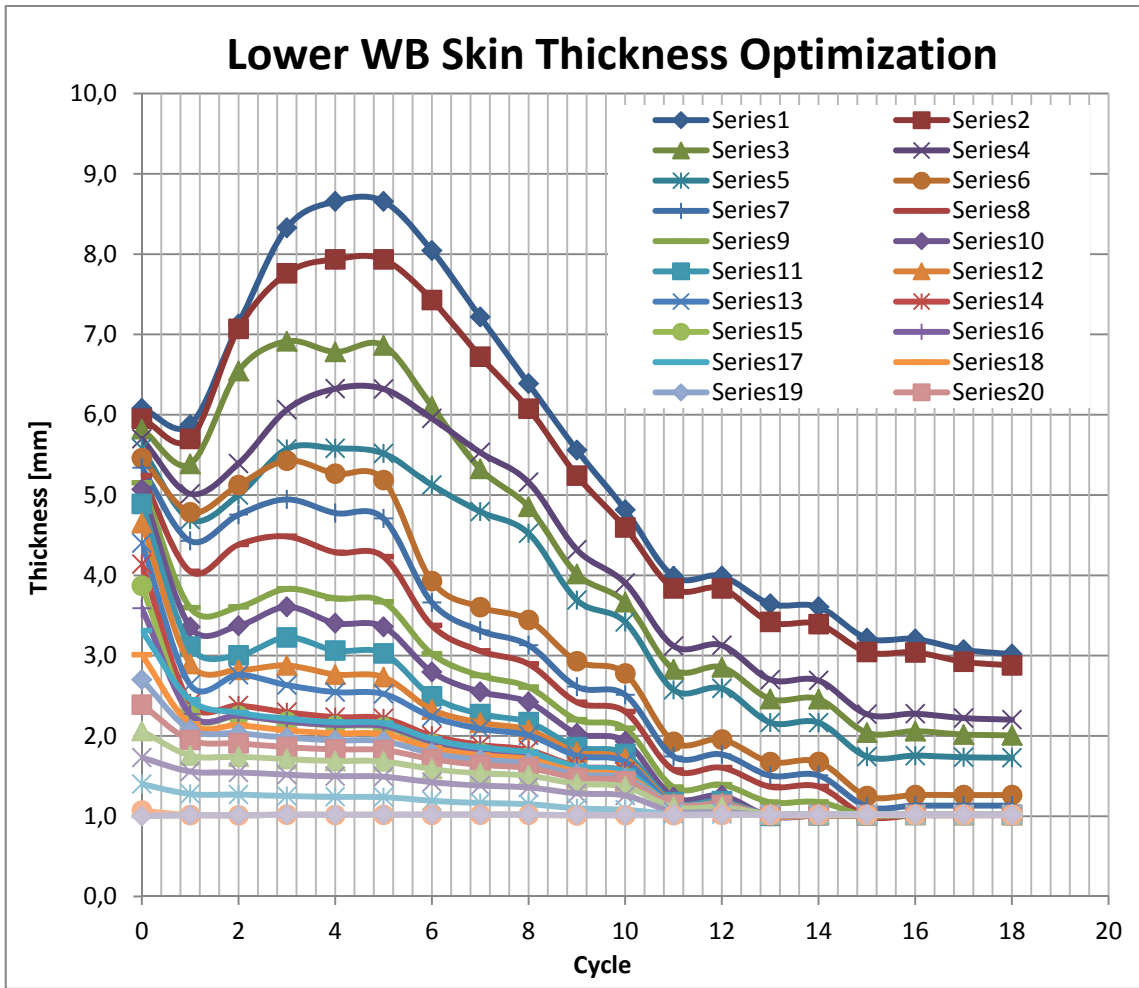


Figure 33 - Lower WB Skin thickness optimization for the 28 sections in Sol200 with stress criterion only for NACA 2420 profile WB, in Static Analysis, 18 cycles total.

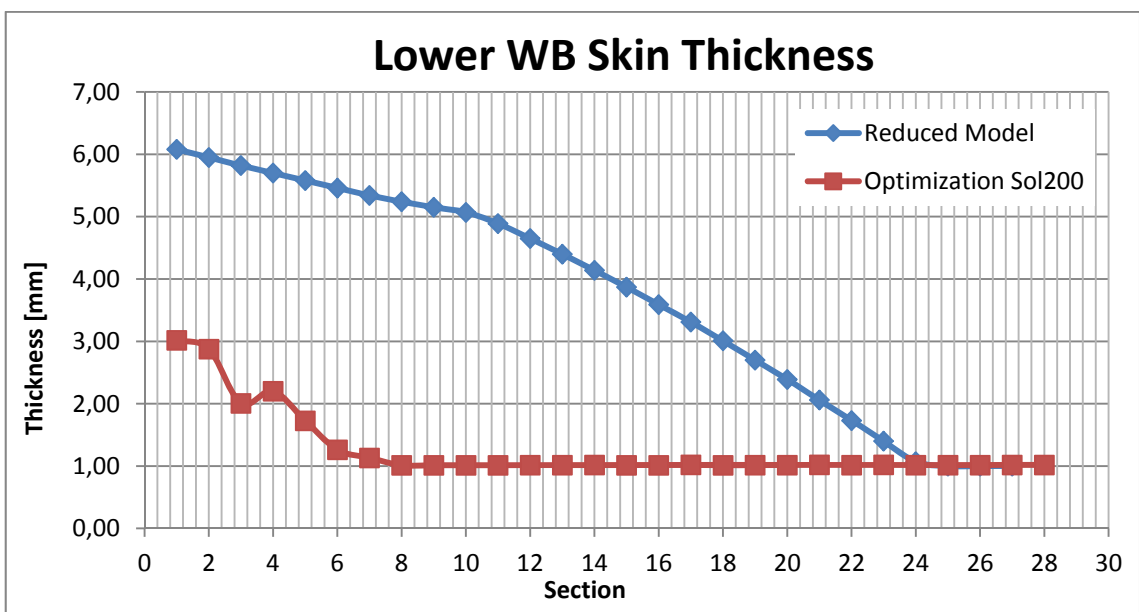


Figure 34 - Lower WB Skin thickness before and after optimization in Sol200 for the 28 sections with stress criterion only for NACA 2420 profile WB, in Static Analysis.

Finally, for the lower WB skin, optimization decreases hugely the overall thickness, and 70% of all sections receive minimum thickness. It's visible that after the optimization, the importance of the lower skin is minimized when considering only stress as criterion, and that is why industry such as Airbus uses fatigue as main design criteria for this structure, instead of stress.

The following pictures show the bending, total displacement and stress tensor on the deformed Wing-Box (real scaling). The maximum vertical wing tip displacement is now 0,412 meters, 77% less than for the non-optimized wing. This reflects the importance of optimization since, in the end, a lighter Wing-Box was generated, with better distributed stress along span, maximum stress respecting the material constraints and a maximum displacement reduced significantly, as may be desirable by aerodynamic constraints. Actually, the maximum displacement criterion isn't usually active when designing a wing, and exists just for a critical reason.

The Total Displacement picture gives the real wing tip displacement dimension, which is much more reasonable than for the non-optimized metallic Wing-Box. Note that these pictures are presented only for quantitative analysis and comparison with the other analysis, and the Upper Skin and Rear Spar are the visible parts.

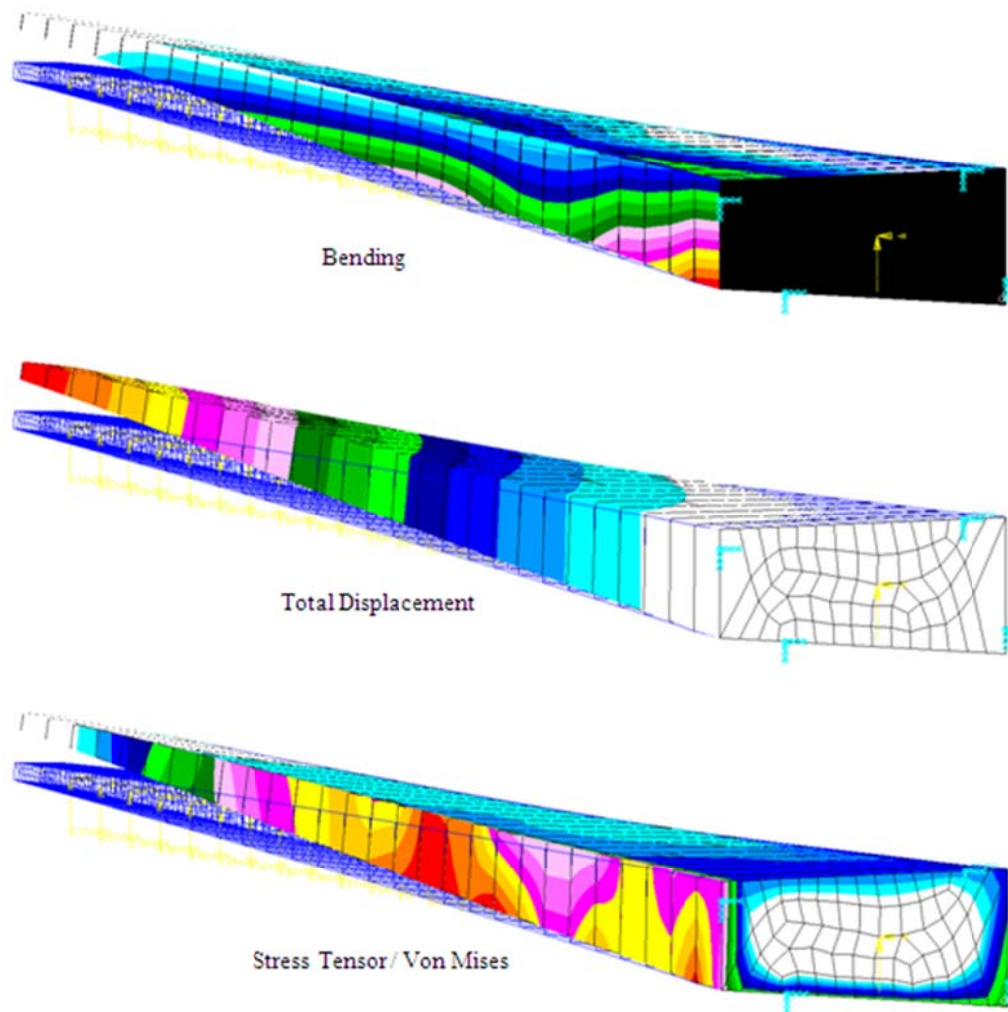


Figure 35 - Bending, Total Displacement and Stress Tensor for NACA 2420 profile WB, Static Analysis optimized by Sol200 with stress criterion only.

As seen, the optimization process gave significant importance to spar, specially the rear spar, minimizing the skin and resulting in a better Wing-Box design, when considering only stress as criterion. More general results for NACA 2415, 3415, 4415, 2420, 2520, 2620, 4420 and 4430 are presented in Annex 1. The numerical results for the optimization of NACA 2420 in Part II are presented in Annex 2.

3.3 - WB optimized by Stress, Strain and Max. Displacement Criteria (Part III)

In this third part, the Wing-Box was optimized by Sol200 based on stress, strain and maximum vertical wing tip displacement criteria, as presented before. This approach is the most complete one, although it does not include the fatigue criterion for the lower WB skin. The 112 thickness variables were redefined to give the minimum global weight respecting all constraints. The other 112 stringers and stiffeners variables were also redefined accordingly to the area relations that define its dependency to the thickness variables. For the NACA 2420, optimization also took 18 cycles to converge, but requested more computational efforts than for Part II. The mass variation can be seen on the picture below.

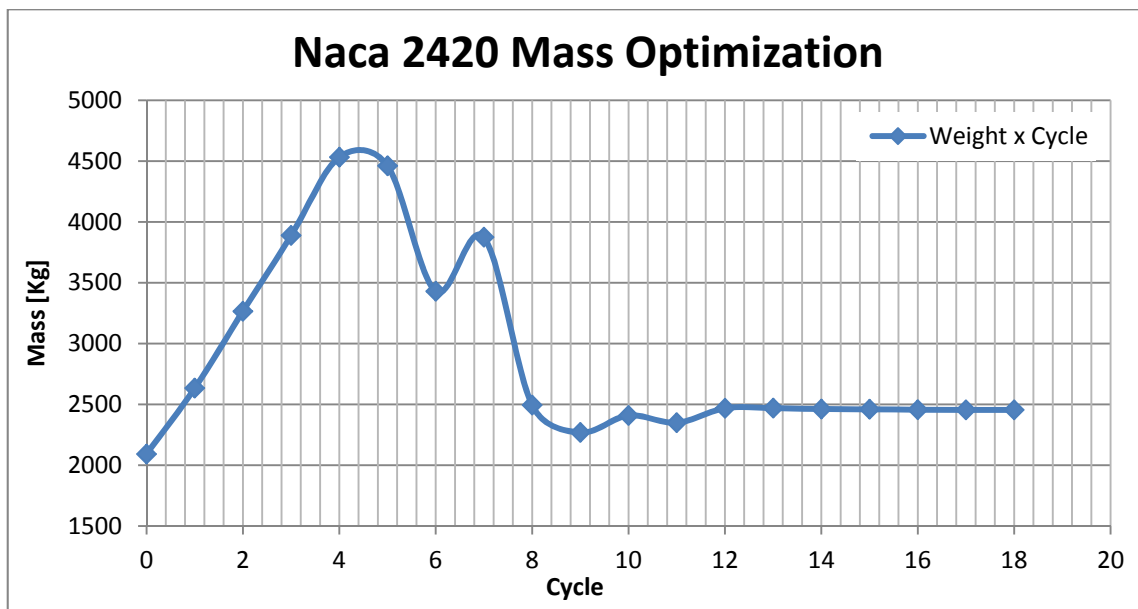


Figure 36 - Mass optimization for NACA 2420 profile WB, Static Analysis optimized by Sol200 with stress, strain and max. displacement criteria, 18 cycles total.

After the 18 cycles, the results converge to a weight of 2454,59 Kg, that is an augmentation of 17,3%. The following table presents the mass in each cycle. The initial mass is 2091,83 Kg.

Table 2 - Mass optimization process in Sol200 for the 18 cycles with stress, strain and max. displacement criteria for NACA 2420 profile WB, in Static Analysis.

Initial Weight 2091.83 Kg.

Cycle	1	2	3	4	5
Total Mass [Kg]	2633,28	3265,29	3888,67	4532,37	4460,57
Cycle	6	7	8	9	10
Total Mass [Kg]	3430,04	3873,92	2494,49	2269,92	2408,90
Cycle	11	12	13	14	15
Total Mass [Kg]	2349,77	2468,64	2469,77	2461,85	2459,99
Cycle	16	17	18	-	-
Total Mass [Kg]	2456,55	2454,59	2454,59	-	-

The exactly same stress criteria as for Part II was used, and the maximum vertical wing tip displacement was of only 0,128 meter, much inferior than the 1,7 meters established by the displacement criteria. Since there was still a mass and rigidity augmentation, it's evident that the strain criterion was decisive when optimizing the structure. The maximum strain adopted was $4 \cdot 10^{-3}$, which is a value allowed only for the best aluminum alloys available nowadays, and increasing this limit would imply on a non-realistic wing.

Now, as for Part II, the optimization results will be presented for each of the four aimed parts: Front Spar, Rear Spar, Upper WB Skin and Lower WB Skin. Each part presents 28 sections (series on the legend), and for each one the thickness optimization for each section will be presented (for the 18 cycles) and also the final thickness along span, before and after optimization.

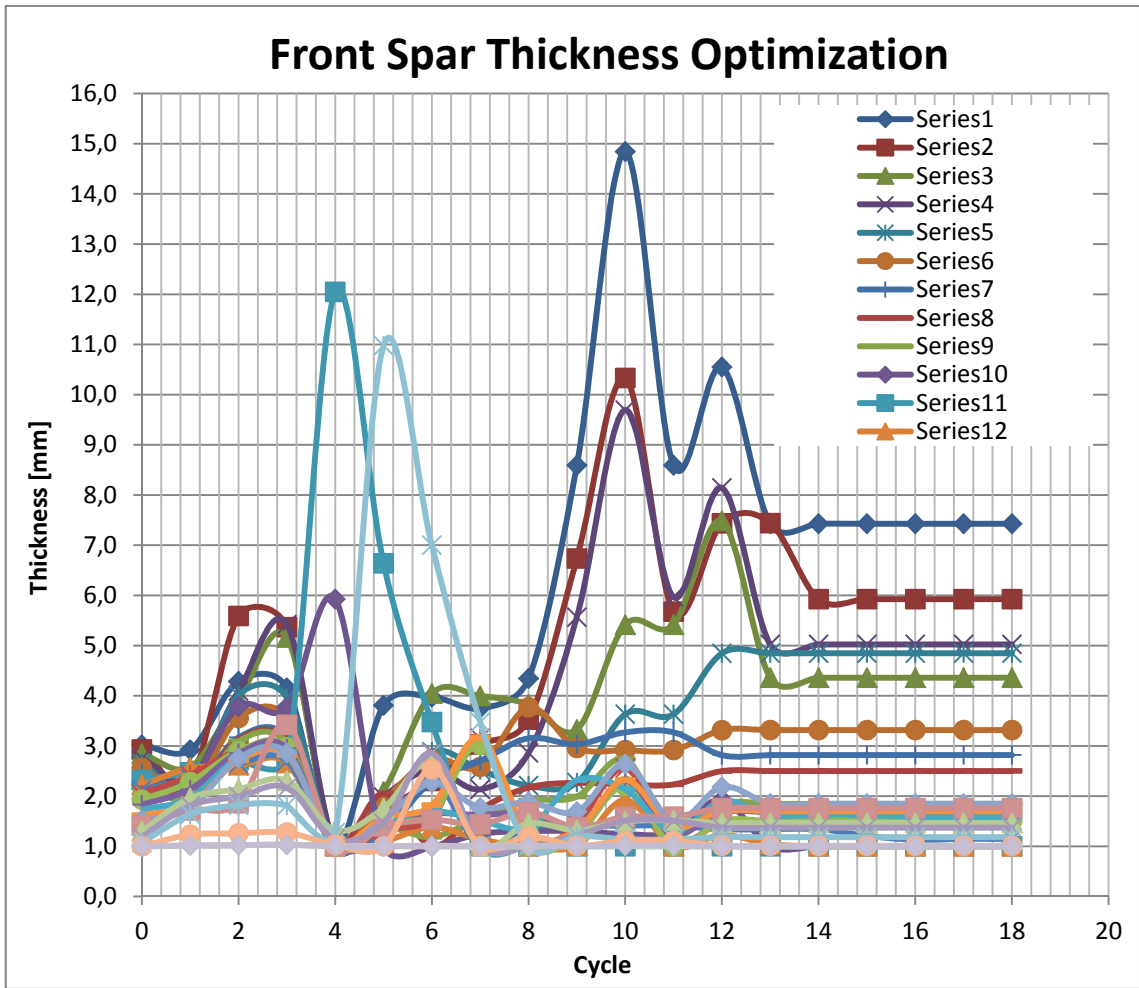


Figure 37 - Front Spar thickness optimization for the 28 sections in Sol200 with stress, strain and max. displacement criteria for NACA 2420 profile WB, in Static Analysis, 18 cycles total.

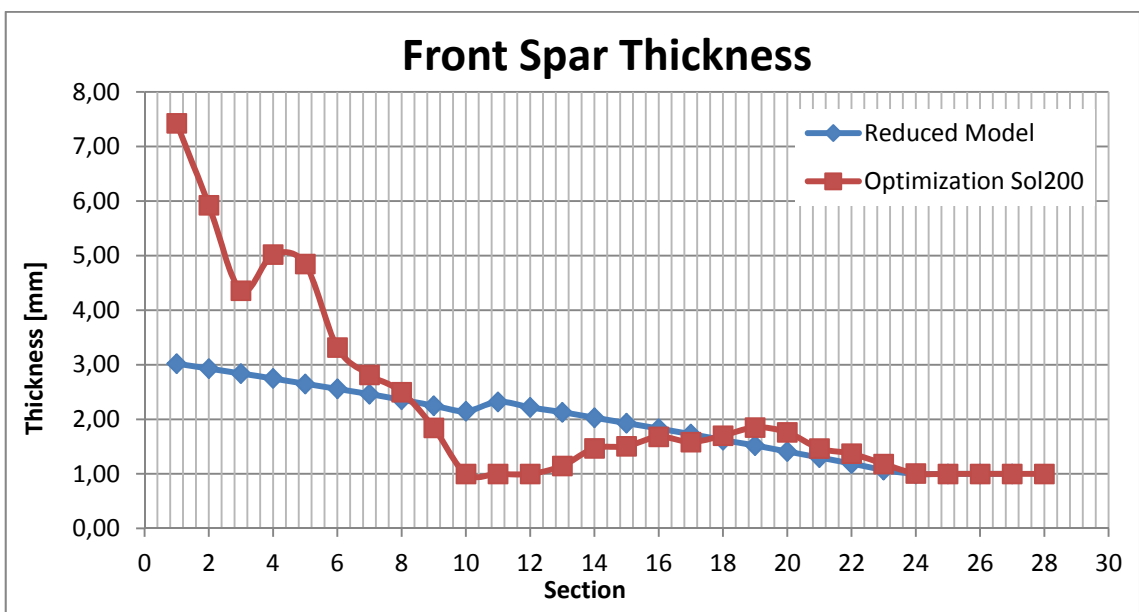


Figure 38 - Front Spar thickness before and after optimization in Sol200 for the 28 sections with stress, strain and max. displacement criteria for NACA 2420 profile WB, in Static Analysis.

For the front spar, the overall thickness was increased up to the 8th section, but the same behavior goes just before the engine, as expected. From the 11th section to the 19th, thickness was decreased and then follows the Reduced Model to the minimum thickness. Globally it's visible that the optimization increased the thickness distribution before the 10th rib, showing that the engine affects greatly the front spar, being decisive when designing this part of the Wing-Box. Although the strain criterion is present, the optimization took a similar path as for Part II;

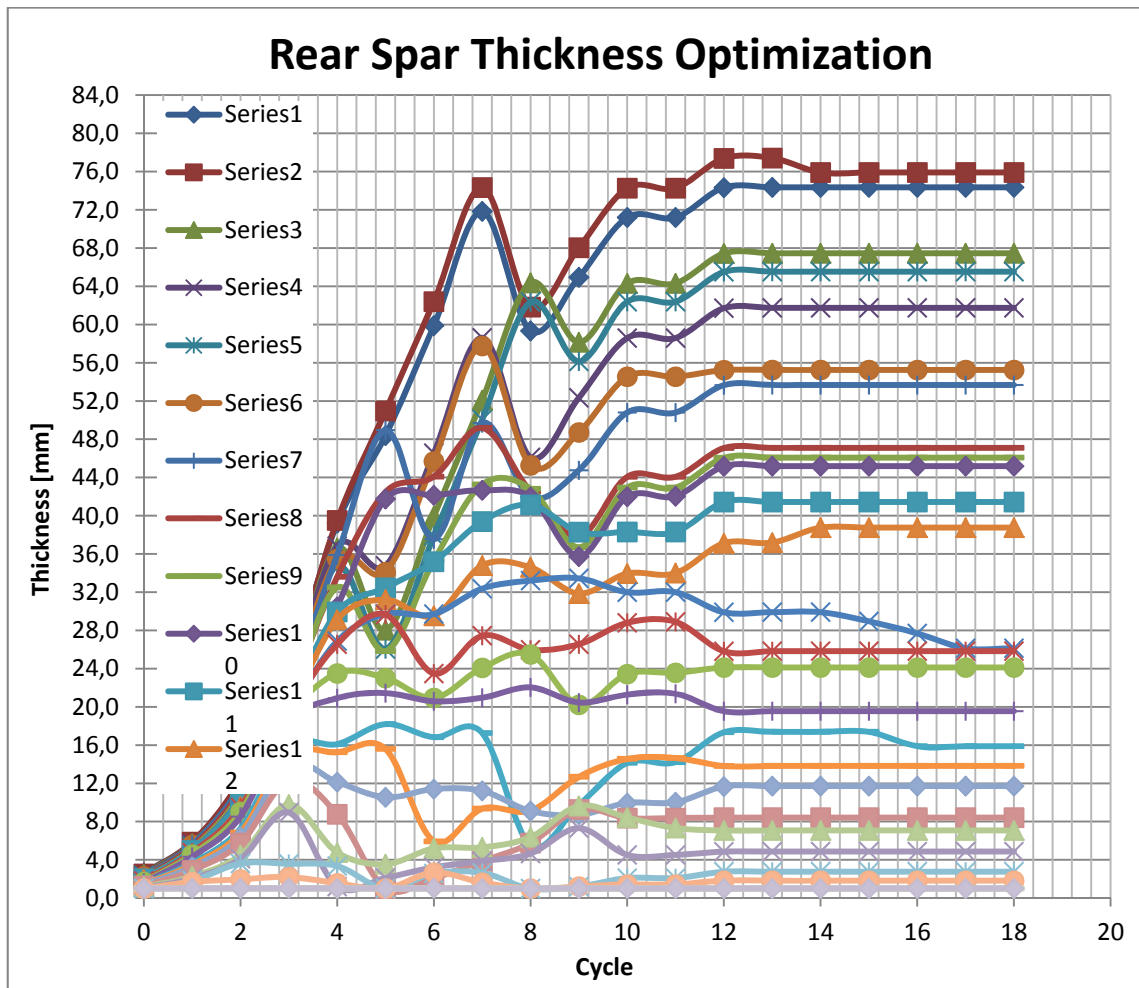


Figure 39 - Rear Spar thickness optimization for the 28 sections in Sol200 with stress, strain and max. displacement criteria for NACA 2420 profile WB, in Static Analysis, 18 cycles total.

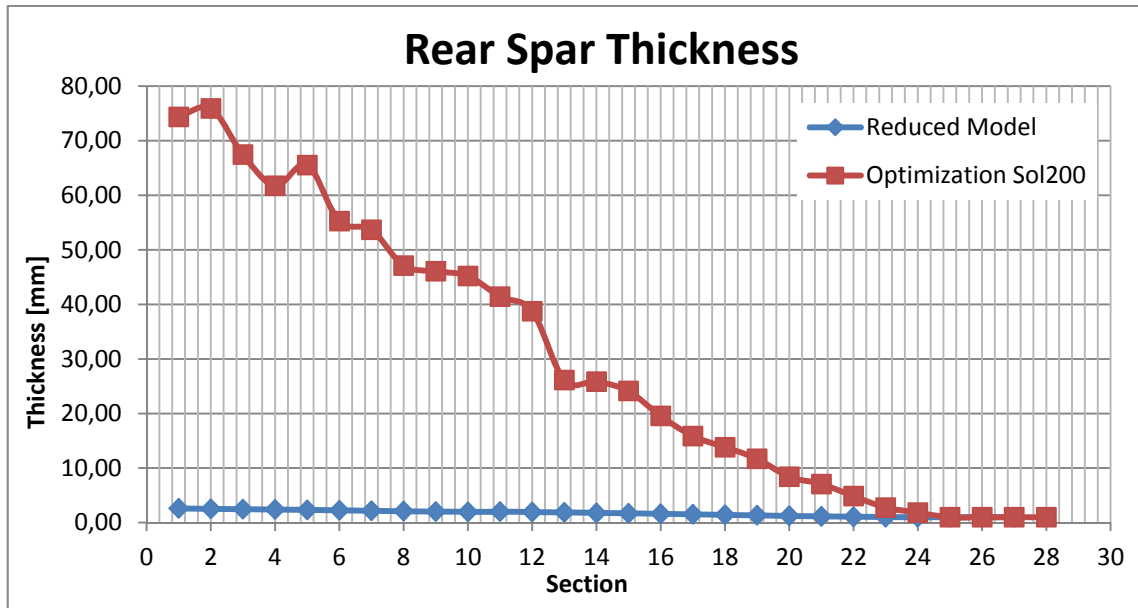


Figure 40 - Rear Spar thickness before and after optimization in Sol200 for the 28 sections with stress, strain and max. displacement criteria for NACA 2420 profile WB, in Static Analysis.

For the rear spar, optimization increased strongly the thickness of every section up to the 24th. The first 5 sections had even an increase of thickness by the order of 30 times, showing that in terms of a globally optimized structure, the rear spar is definitely not well designed by the analytical model. It's important to remember again that the numerical solution considers the interaction between all elements of the model, and so the response may be extremely different than expected. After optimization, the rear spar is totally different than the initial structure, and the thickness distribution along span is more linear than for Part II.

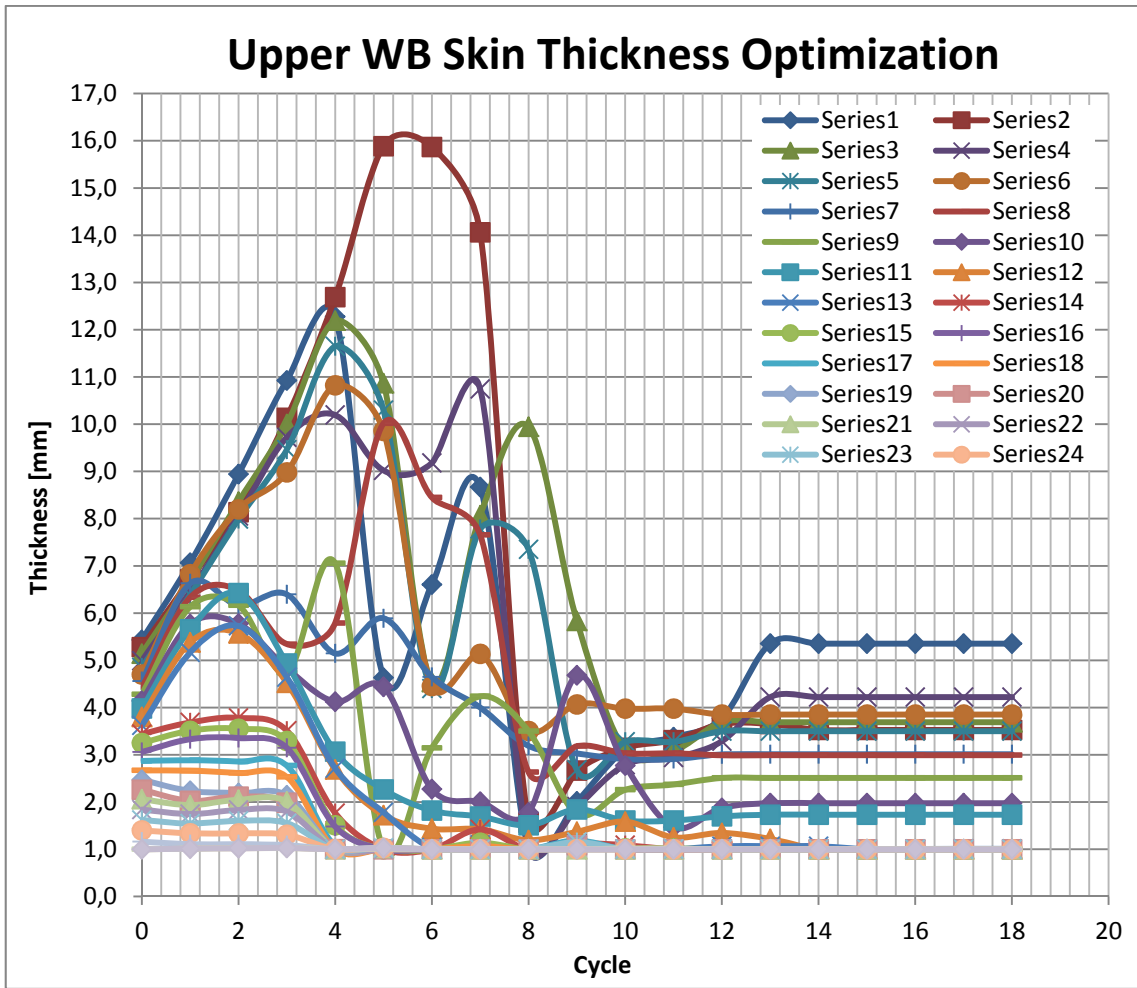


Figure 41 - Upper WB Skin thickness optimization for the 28 sections in Sol200 with stress, strain and max. displacement criteria for NACA 2420 profile WB, in Static Analysis, 18 cycles total.

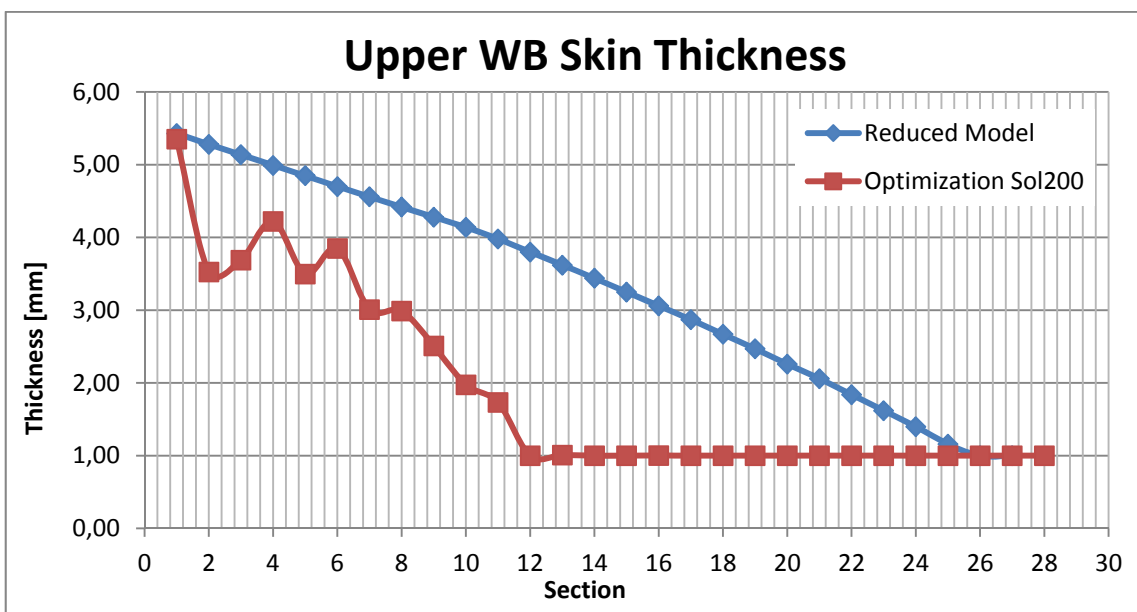


Figure 42 - Upper WB Skin thickness before and after optimization in Sol200 for the 28 sections with stress, strain and max. displacement criteria for NACA 2420 profile WB, in Static Analysis.

The behavior of the upper WB skin is again completely different from the spars. There was a considerable increase of thickness just after the engine, and from the 12th section up to the wing tip, thickness was lowered to the minimum value. This shows how diminished is the importance of the upper WB skin after the optimization of the spar, which takes almost all efforts by the end of the optimization. Nevertheless, it's possible to see the influence of the engine on the upper WB skin design, although the spars support almost all efforts after optimization.

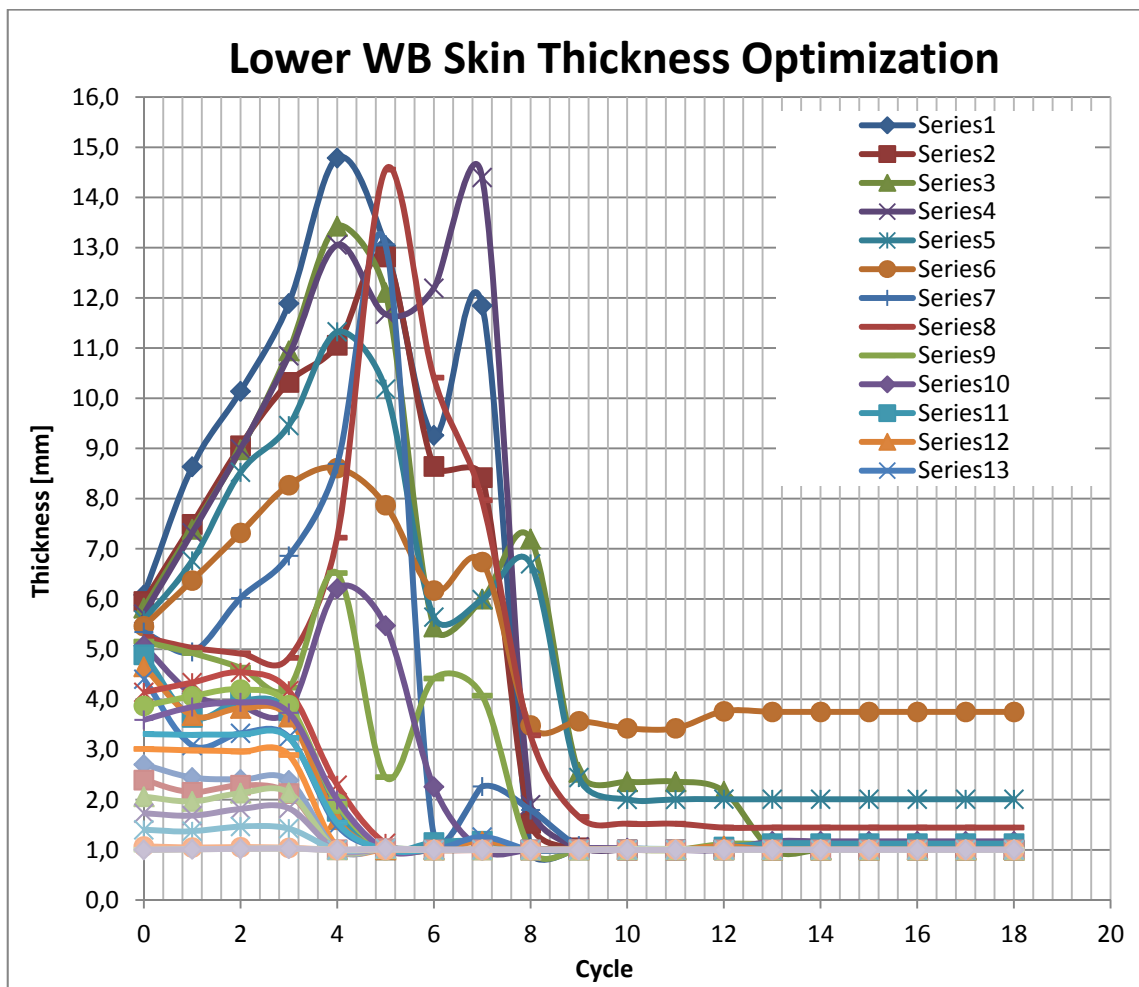


Figure 43 - Lower WB Skin thickness optimization for the 28 sections in Sol200 with stress, strain and max. displacement criteria for NACA 2420 profile WB, in Static Analysis, 18 cycles total.

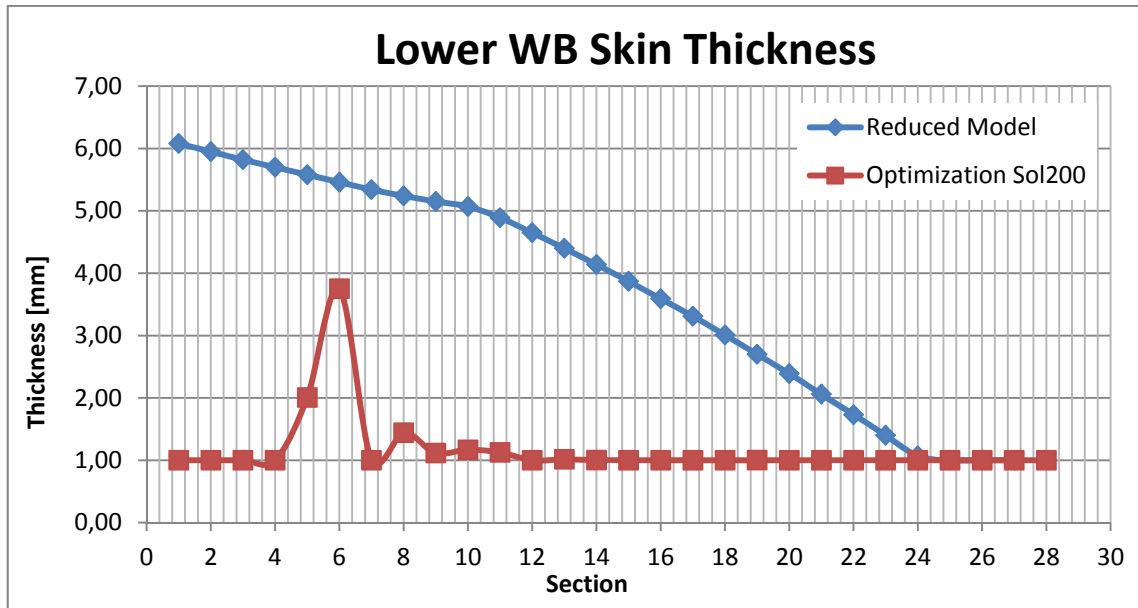


Figure 44 - Lower WB Skin thickness before and after optimization in Sol200 for the 28 sections with stress, strain and max. displacement criteria for NACA 2420 profile WB, in Static Analysis.

Finally, for the lower WB skin, optimization decreases totally the overall thickness to minimum (sections 5 and 6 may present a numerical error). It's visible that after the optimization, the importance of the lower skin is absolutely minimized, remembering why industry uses fatigue as main design criteria for this part, not forgetting that the Wing-Box is a closed section structure and must remain this way to keep the overall aerodynamic shape of the profile.

The following pictures show the bending, total displacement and stress tensor on the deformed Wing-Box (real scaling). The maximum vertical wing tip displacement is now, as said before, of only 0,128 meters, 94% less than for the non-optimized wing. The Total Displacement picture gives the real wing tip displacement dimension, which is again much more reasonable than for the non-optimized Wing-Box. Note that these pictures are presented only for quantitative analysis and comparison with the other analysis, and the Upper Skin and Rear Spar are the visible parts.

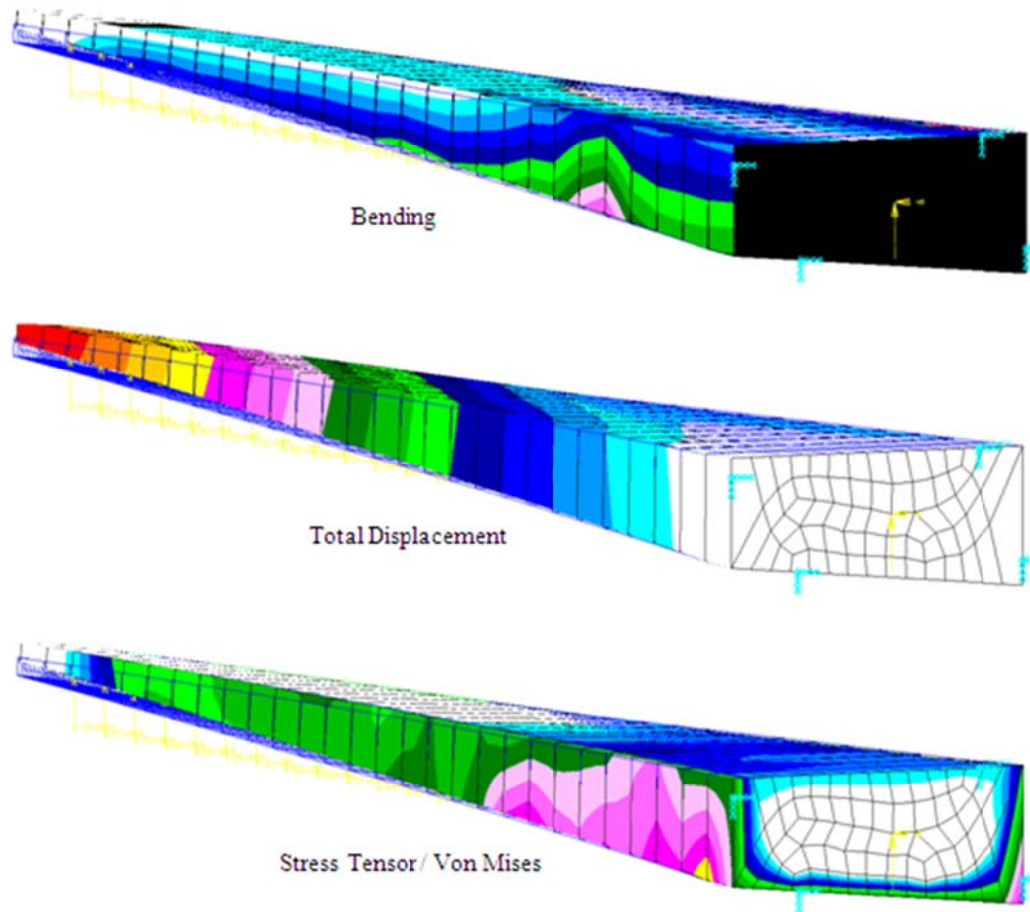


Figure 45 - Bending, Total Displacement and Stress Tensor for NACA 2420 profile WB, Static Analysis optimized by Sol200 with stress, strain and max. displacement criteria.

The numerical results for the optimization of NACA 2420 in Part III are presented in Annex 3.

4 - Conclusion

This report presented the highlights of this work conducted in four months. The construction of an all parameterized Wing-Box in PCL Code showed to be extremely useful, since the objective of the project was to analyze a great number of different structures, and reconstructing a new model was possible in only a few minutes. Although Patran is a nice GUI interface for Nastran, structures with a large number of nodes and elements may be easier constructed with aid of other programs such as Excel or Matlab, since the PCL code might overpass thousands of lines.

The optimization process in Sol200 also showed to be more complex than expected. Nastran has an enormous capability of calculation, but has also its limitation as could be seen when trying to define a property optimization with a non-linear relation. Nevertheless, the response was better than expected, and results were satisfactory.

It was visible that the stress criterion is not a good choice when designing the lower WB skin, remembering why industry uses fatigue as main design criteria for this part. The maximum vertical wingtip displacement also showed to be useless when strain and/or stress criteria are also adopted. Finally, strain proved to be much stronger than stress in this type of analysis, so industry might adopt it in a different approach or with some modifications on the stress criteria.

After the optimization, the importance of upper and lower skins was minimized and almost all efforts were concentrated on spars, specially the rear spar. This makes us think if it's not possible to create a simple WB model with only one or two beams and still have good approximate results, just for preliminary analysis.

A deeper step is to associate this work with an aerodynamic approach using CFD, optimizing the structure accordingly to its aerodynamic response, since when in cruise, the deformed wing may request a new shape for the best efficiency. In this way, it would be possible to create a variation of the required profile to construct the real wing that, when deformed, would assume its best shape in terms of aerodynamics, still respecting all structural constraints and minimum weight possible.

Another important approach is to do the exactly same study but with composite materials, since the future of aviation may reside no more in metallic alloys, but in composites. The optimization of composite plates and shells, although, requests a much greater computational effort, since thickness is no longer the only variable, but also the number of layer and its orientation.

Finally, the parametric model approach for structural optimization of a flexible wing, together with the reduced model, is a useful tool for the preliminary design of wing-boxes, helping the preliminary design task to achieve the optimized structure in the shortest time, enhancing the results by the lowest costs possible.

5 - References

- [1] LIMA, Erick Assis. **Structural Optimization of a Flexible Wing: Reduced Model Approach**. Instituto Tecnológico de Aeronáutica & Intitut Supérieur de l'Aéronautique et de l'Espace, July 2011.
- [2] MSC. Software Corporation. **MD R2 Nastran Quick Reference Guide**. 2007.
- [3] MSC. Software Corporation, **MD Nastran 2010 Design Sensitivity and Optimization User's Guide**. 2010.
- [4] MSC. Software Corporation. **NAS107 Workshop for MSC.Nastran 2001 and MSC. Patran 2001.r3**. April 2003.
- [5] MSC. Software Corporation, **NX Nastran Error List**. 2005.
- [6] MSC. Software Corporation. **PATRAN 304 Exercise Workbook**.
- [7] MSC. Software Corporation. **PAT302 Workshop 19, 20 and 21: Glogal/Local modeling using FEM fields, Create PCL Functions and PCL via session file**. Decembre 2004.
- [8] ROUX Elodie. **Modèle de Masse Voilure Avions de transport civil pour une approche analytique de la Dynamique du Vol**. Intitut Supérieur de l'Aéronautique et de l'Espace - Supaero & ONERA, 2006.
- [9] MEGSON T.H.G. **Aircraft Structures for engineering students**. Butterworth Heinemann, 3rd Edition, 1999.
- [10] JOHNSON, Erwin H. **Fully Stressed Design in MSC.Nastran**. MSC.Software Corporation, Paper No. 2001-42, 2001.
- [11] JENCKINSON Lloyd R.; MARCHMAN III James F. **Aircraft Design Projects for engineering students**. Butterworth Heinemann, 2003.

- [12] MORLIER J.; FRANCOIS A.; ABDULLAH E. **Initiation à PATRAN/NASTRAN pour le calcul des structures.** Intitut Supérieur de l'Aéronautique et de l'Espace, Version 2.0, 2010.
- [13] MORLIER J. **Workshop 0: Simple Stress analysis of a solid.** Intitut Supérieur de l'Aéronautique et de l'Espace, 2010.
- [14] MORLIER J. **Workshop 1: I Beam static analysis.** Intitut Supérieur de l'Aéronautique et de l'Espace, 2010.
- [15] MORLIER J. **Workshop 2: I Lecture/edition du fichier bdf.** Intitut Supérieur de l'Aéronautique et de l'Espace, 2010.
- [16] HURLIMANN Florian. **Mass Estimation of Transport Aircraft Wing-Box Structures with a CAD/CAE - Based Multidisciplinary Process.** ETH Zurich, Diss ETH No 19458, 2010.
- [17] RAO J. S.; KIRAN S.; CHANDRA Satish; KAMESH J.V.; PADMANABHAN Madhusudan A. **Topology Optimization of Aircraft Wing.** HTC08, 2008.
- [18] NIEMANN Hanno. **A simple Topology Optimization Example with MD R2 Patran.** Intitut Supérieur de l'Aéronautique et de l'Espace - Supaero & IFL TU Braunschweig, 2008.
- [19] RAGHY, Engr Sreejit. **Finite Element Modeling Techniques in MSC. NASTRAN and LS/DYNA.** Ove Arup & Partners International Ltd, 2nd Edition, November 2009.
- [20] ALDEBERT Gregory; BONNAFFE Jean-Louis; DAS NEVES Mickael; RICHARD Arnaud. **Dimensionnement d'une aile d'Airbus A320.** ESTACA Ecole d'Ingenieurs, 2007.
- [21] SHI. G.; RENAUD. G.; YANG X.; ZHANG F.; CHEN S. **Integrated Wing Design with Three Disciplines.** AIAA 2002-5405, September 2002.

[22] MOSTAFA S. A.; SINGH Amandeep; SEDAGHATI Ramin. **Conceptual Design Optimization of an Aircraft Wing-Box Structure and Generating a High Fidelity Stick Model**. DMIE Concordia University, Report 6, 2007.

[23] École Polytechnique de Montréal. **Cours MEC3400**. Département de Génie Mécanique, 2008.

[24] MORLIER J. **Optimisation de structures : Algorithmes pour l'optimisation numérique**. Intitut Supérieur de l'Aéronautique et de l'Espace, February 2010.

Annex 1 - More optimization results for Part II (8 NACA Profiles)

In this annex, more general results for NACA 2415, 3415, 4415, 2420, 2520, 2620, 4420 and 4430 are presented, using the same optimization method as for Part II. The table below presents the final weight for each of the 8 Wing-Box studied

Table 3 - Mass optimization in Sol200 for the 8 studied WB with different NACA profiles with stress criterion only in Static Analysis.

NACA	2415	3415	4415	2420	2520	2620	4420	4430
Wing Semi-Span [m]	38,3	34,2	31,2	38,3	37,4	36,2	31,2	31,2
Initial Mass [Kg]	2361,4	2148,0	2124,0	2091,8	2001,1	1883,8	1641,2	1407,5
Final Mass [Kg]	1551,9	1343,0	1096,2	1805,9	1729,0	1620,0	1244,3	1510,9
Reduction [%]	-34,3	-37,5	-48,4	-13,7	-13,6	-14,0	-24,2	7,3

The quadratic mean of mass reduction for the 8 studied NACA profile is 26,1%, which is a great result since aeronautical industry searches the weight minimization at all costs. This study was conducted in order to provide a response tool to the Reduced Model, and a much deeper analysis about the influence of NACA parameters on global wing weight can be found on reference [2].

As an exception for NACA 4430, the optimizations of the other 7 models follow the weight order that means the wings before and after optimization keep the same position in terms of final mass. Since all WB were design for corresponding wing with the same total lift coefficient, it's visible that the NACA 4420 is the best chosen wing when considering lift/weight. In fact, the profile NACA 4420 has a good thickness ratio and a considerable maximum camber, being very similar to the profiles uses in commercial aircrafts (e.g. Airbus A320 wing uses a variation of NACA 4412 profile).

It's also possible to see that increasing the maximum camber position in NACA 2X20 series decreases the weight, and the same when increasing the maximum camber in NACA X415 series. That explains in parts why NACA 44XX is the best choice for this type of aircraft, since both maximum camber and maximum camber position are high enough and almost at the limit of NACA 4-Digits Series equations.

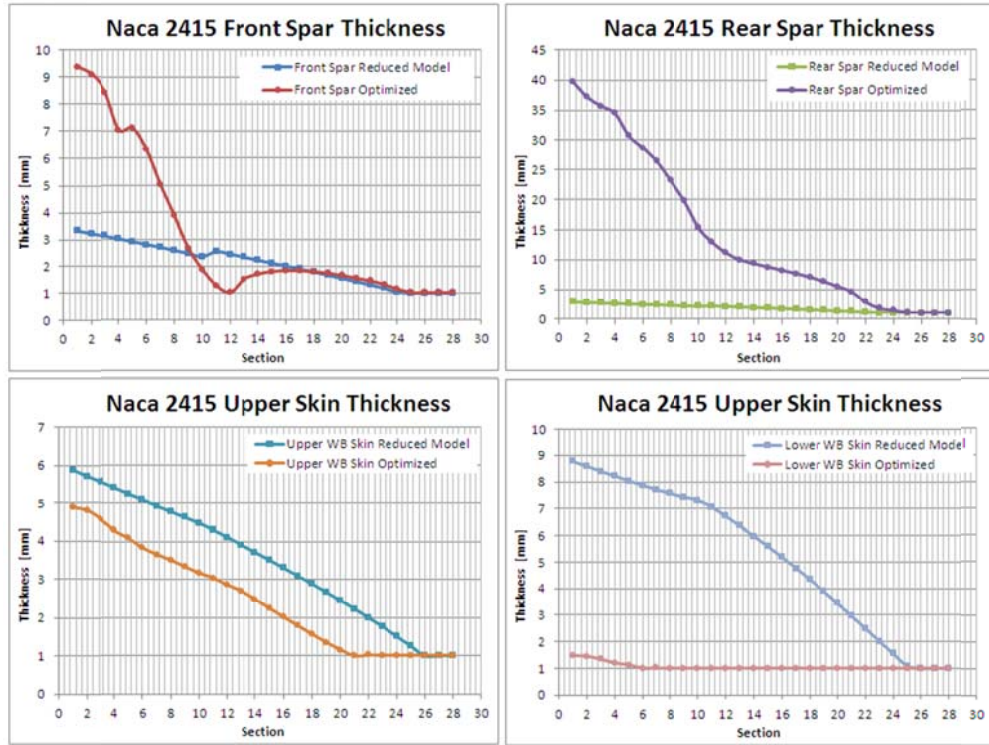


Figure 46 - NACA 2415 profile WB optimized by Sol200 with stress criterion only, Statics Analysis. Final thickness for Front and Rear Spars, Upper and Lower WB Skins.

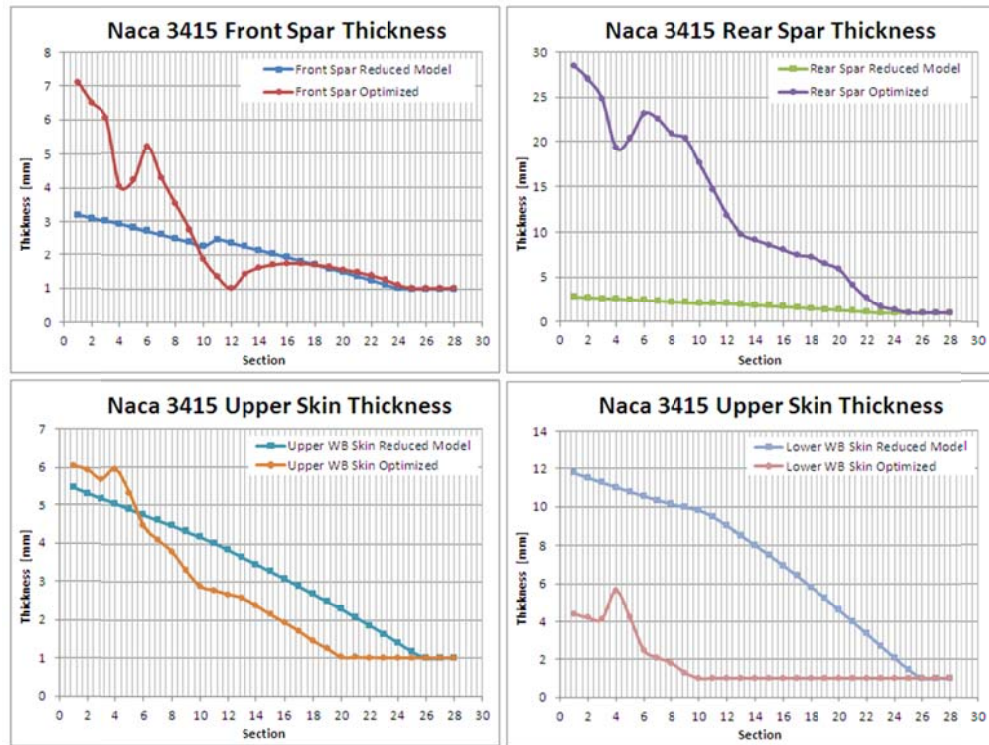


Figure 47 - NACA 3415 profile WB optimized by Sol200 with stress criterion only, Statics Analysis. Final thickness for Front and Rear Spars, Upper and Lower WB Skins.

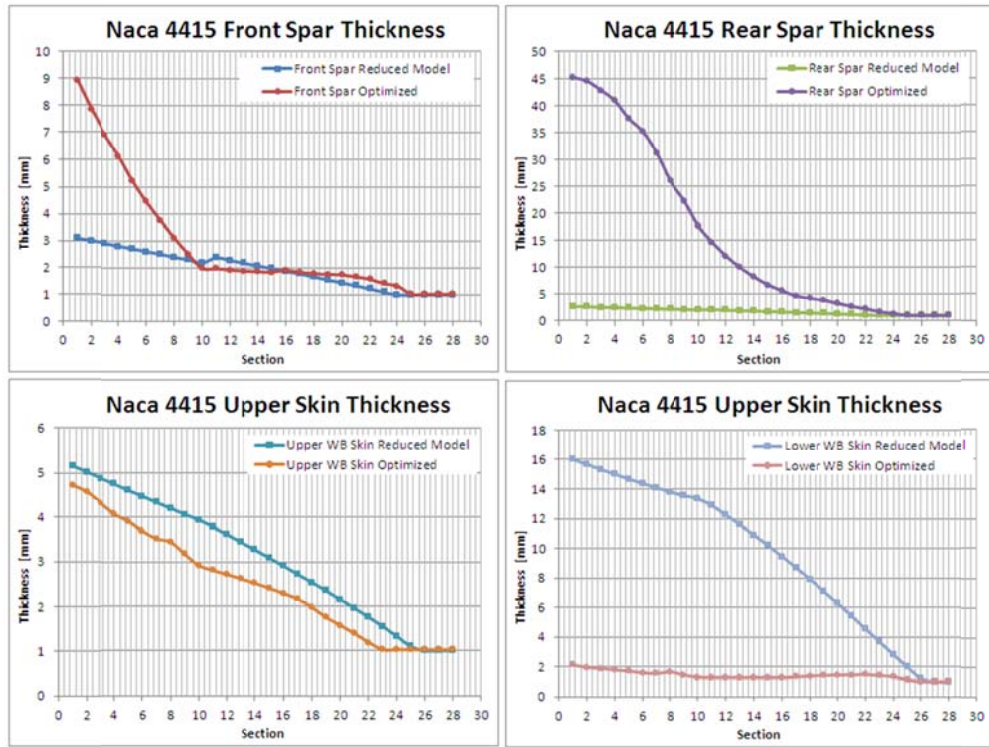


Figure 48 - NACA 4415 profile WB optimized by Sol200 with stress criterion only, Statics Analysis. Final thickness for Front and Rear Spars, Upper and Lower WB Skins.

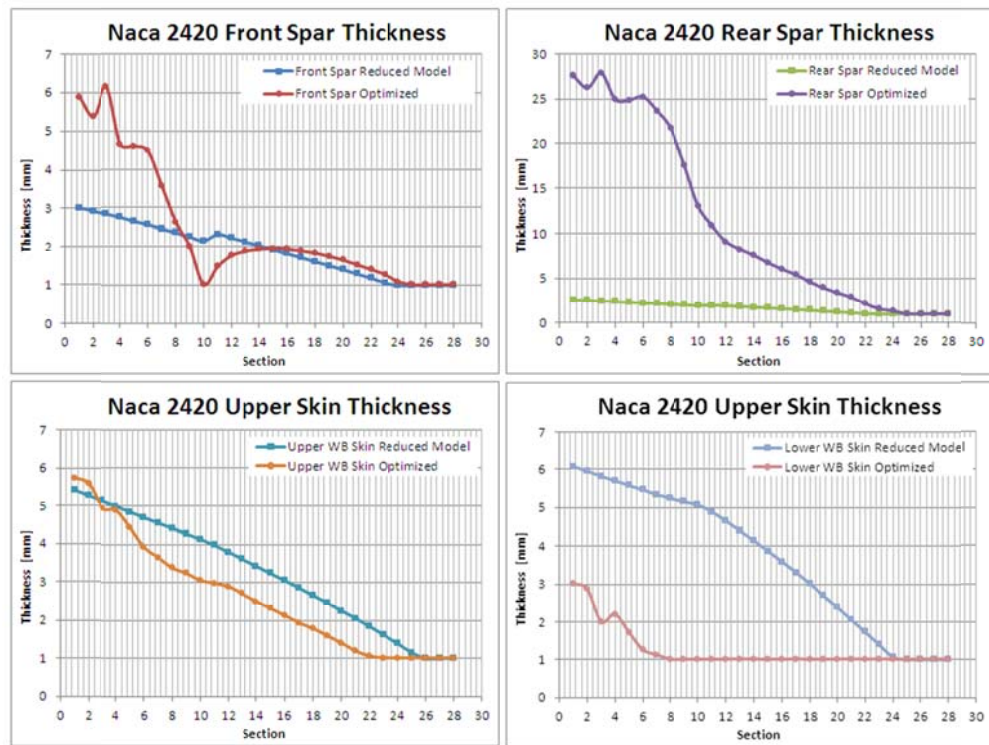


Figure 49 - NACA 2420 profile WB optimized by Sol200 with stress criterion only, Statics Analysis. Final thickness for Front and Rear Spars, Upper and Lower WB Skins.

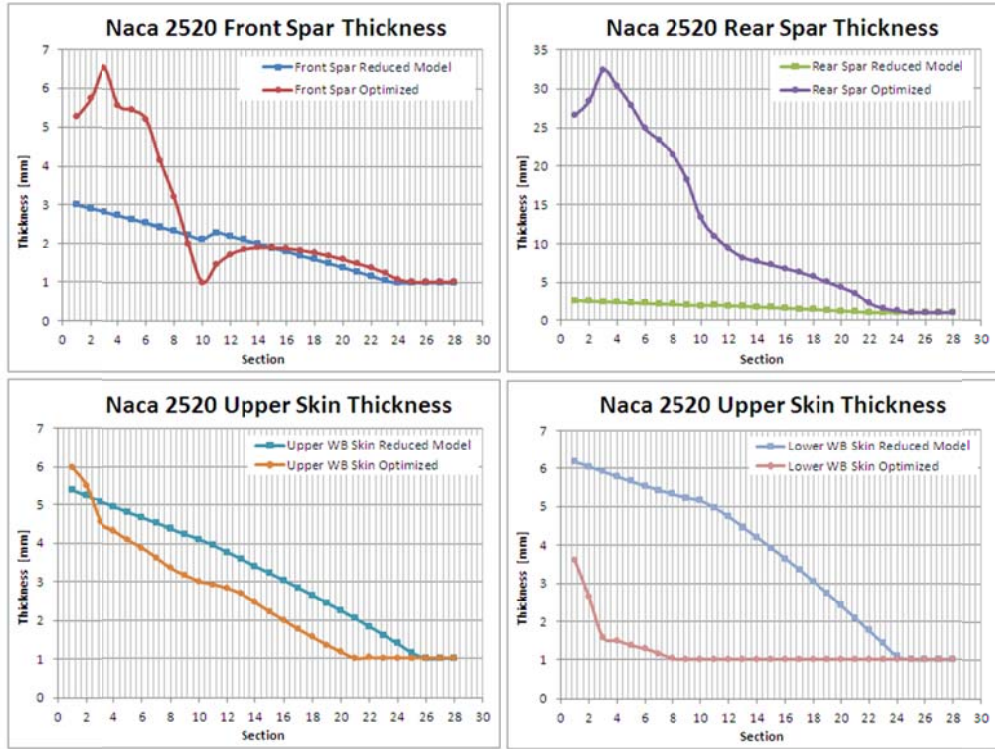


Figure 50 - NACA 2520 profile WB optimized by Sol200 with stress criterion only, Statics Analysis. Final thickness for Front and Rear Spars, Upper and Lower WB Skins.

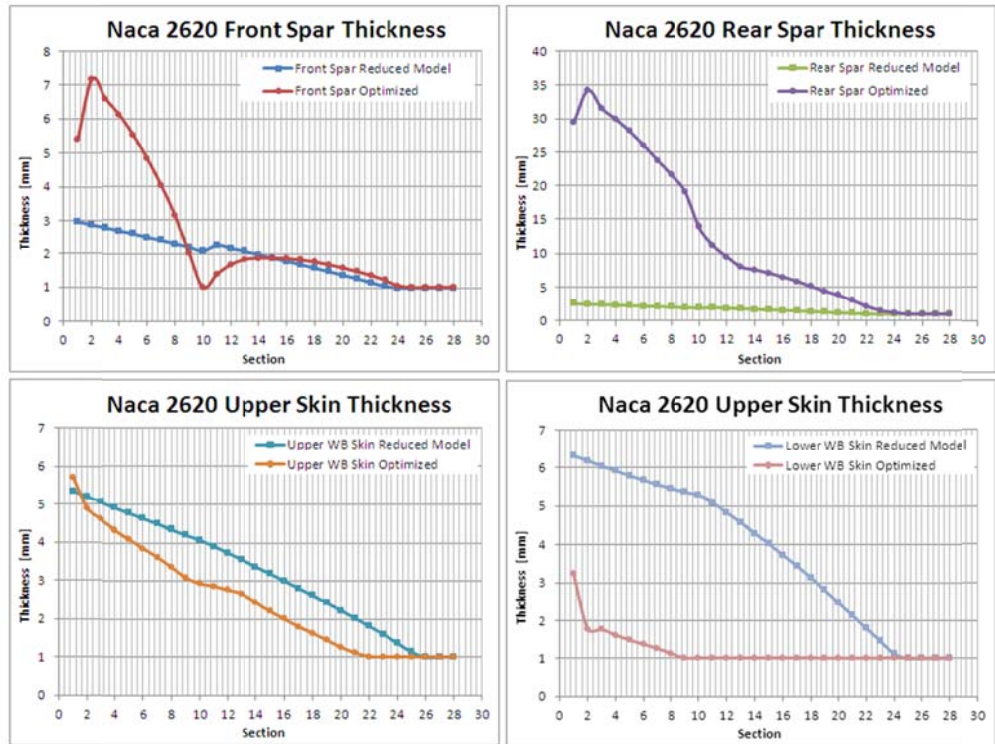


Figure 51 - NACA 2620 profile WB optimized by Sol200 with stress criterion only, Statics Analysis. Final thickness for Front and Rear Spars, Upper and Lower WB Skins.

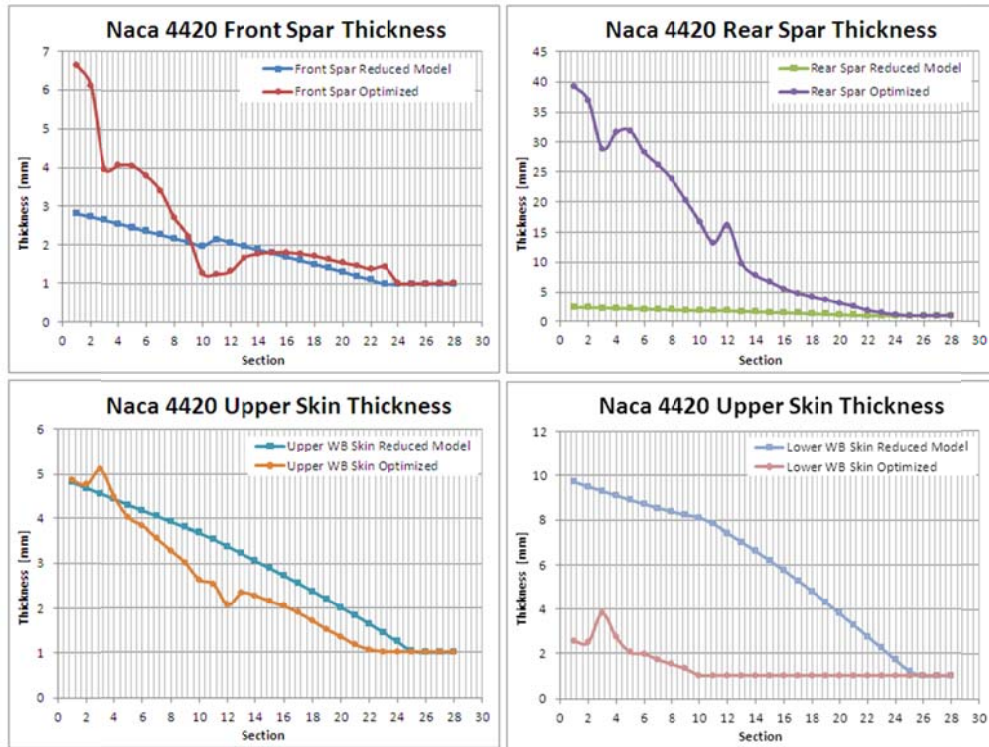


Figure 52 - NACA 4420 profile WB optimized by Sol200 with stress criterion only, Statics Analysis. Final thickness for Front and Rear Spars, Upper and Lower WB Skins.

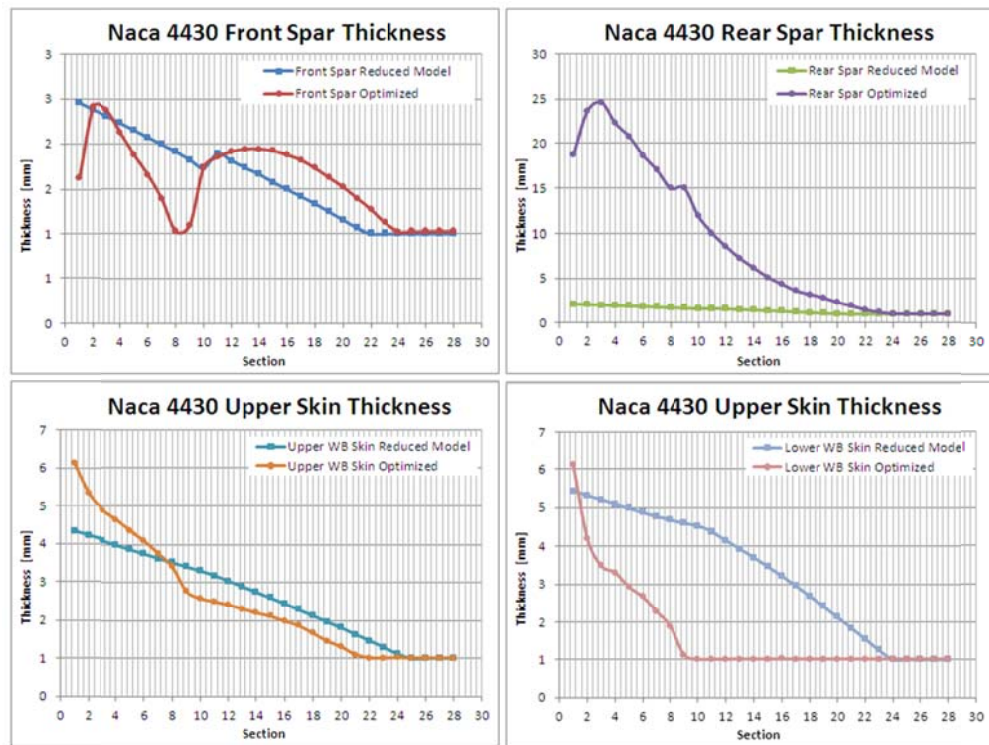


Figure 53 - NACA 2430 profile WB optimized by Sol200 with stress criterion only, Statics Analysis. Final thickness for Front and Rear Spars, Upper and Lower WB Skins.

Annex 2 - Numerical results for Part II optimization

Table 4 - Numerical results for the thickness optimization in Sol200 of NACA 2420 profile WB with stress criterion only, in Static Analysis. Front Spar Part II.

Section	Name	Initial Thickness [mm]	Final Thickness [mm]
FRONT SPAR [Part II]			
1	Front Spar 1	3,02	7,43
2	Front Spar 2	2,93	5,93
3	Front Spar 3	2,84	4,36
4	Front Spar 4	2,75	5,02
5	Front Spar 5	2,65	4,85
6	Front Spar 6	2,56	3,32
7	Front Spar 7	2,46	2,82
8	Front Spar 8	2,36	2,50
9	Front Spar 9	2,25	1,84
10	Front Spar 10	2,15	1,00
11	Front Spar 11	2,32	1,00
12	Front Spar 12	2,22	1,00
13	Front Spar 13	2,13	1,15
14	Front Spar 14	2,03	1,47
15	Front Spar 15	1,93	1,51
16	Front Spar 16	1,83	1,68
17	Front Spar 17	1,73	1,58
18	Front Spar 18	1,62	1,70
19	Front Spar 19	1,52	1,85
20	Front Spar 20	1,41	1,76
21	Front Spar 21	1,30	1,47
22	Front Spar 22	1,19	1,37
23	Front Spar 23	1,07	1,18
24	Front Spar 24	1,00	1,01
25	Front Spar 25	1,00	1,00
26	Front Spar 26	1,00	1,00
27	Front Spar 27	1,00	1,00
28	Front Spar 28	1,00	1,00

Table 5 - Numerical results for the thickness optimization in Sol200 of NACA 2420 profile WB with stress criterion only, in Static Analysis. Rear Spar Part II.

Section	Name	Initial Thickness [mm]	Final Thickness [mm]
REAR SPAR			
1	Rear Spar 1	2,60	27,59
2	Rear Spar 2	2,53	26,25
3	Rear Spar 3	2,46	27,85
4	Rear Spar 4	2,39	24,97
5	Rear Spar 5	2,32	24,89
6	Rear Spar 6	2,25	25,26
7	Rear Spar 7	2,18	23,68
8	Rear Spar 8	2,10	21,70
9	Rear Spar 9	2,03	17,55
10	Rear Spar 10	1,95	12,98
11	Rear Spar 11	2,01	10,79
12	Rear Spar 12	1,94	9,06
13	Rear Spar 13	1,86	8,25
14	Rear Spar 14	1,77	7,57
15	Rear Spar 15	1,69	6,75
16	Rear Spar 16	1,61	6,02
17	Rear Spar 17	1,52	5,41
18	Rear Spar 18	1,43	4,57
19	Rear Spar 19	1,34	3,94
20	Rear Spar 20	1,25	3,38
21	Rear Spar 21	1,15	2,90
22	Rear Spar 22	1,05	2,17
23	Rear Spar 23	1,00	1,58
24	Rear Spar 24	1,00	1,36
25	Rear Spar 25	1,00	1,02
26	Rear Spar 26	1,00	1,02
27	Rear Spar 27	1,00	1,02
28	Rear Spar 28	1,00	1,02

Table 6 - Numerical results for the thickness optimization in Sol200 of NACA 2420 profile WB with stress criterion only, in Static Analysis. Upper Skin Part II.

Section	Name	Initial Thickness [mm]	Final Thickness [mm]
UPPER SKIN			
1	Upper Skin 1	5,43	5,75
2	Upper Skin 2	5,28	5,60
3	Upper Skin 3	5,14	4,95
4	Upper Skin 4	4,99	4,89
5	Upper Skin 5	4,85	4,44
6	Upper Skin 6	4,70	3,93
7	Upper Skin 7	4,56	3,66
8	Upper Skin 8	4,42	3,39
9	Upper Skin 9	4,28	3,25
10	Upper Skin 10	4,14	3,07
11	Upper Skin 11	3,98	2,99
12	Upper Skin 12	3,80	2,90
13	Upper Skin 13	3,62	2,71
14	Upper Skin 14	3,44	2,51
15	Upper Skin 15	3,25	2,33
16	Upper Skin 16	3,06	2,14
17	Upper Skin 17	2,87	1,95
18	Upper Skin 18	2,67	1,79
19	Upper Skin 19	2,47	1,60
20	Upper Skin 20	2,26	1,41
21	Upper Skin 21	2,06	1,20
22	Upper Skin 22	1,84	1,07
23	Upper Skin 23	1,62	1,02
24	Upper Skin 24	1,40	1,02
25	Upper Skin 25	1,16	1,02
26	Upper Skin 26	1,00	1,02
27	Upper Skin 27	1,00	1,02
28	Upper Skin 28	1,00	1,02

Table 7 - Numerical results for the thickness optimization in Sol200 of NACA 2420 profile WB with stress criterion only, in Static Analysis. Lower Skin Part II.

Section	Name	Initial Thickness [mm]	Final Thickness [mm]
LOWER SKIN			
1	Lower Skin 1	6,08	3,02
2	Lower Skin 2	5,95	2,88
3	Lower Skin 3	5,82	2,01
4	Lower Skin 4	5,70	2,20
5	Lower Skin 5	5,58	1,73
6	Lower Skin 6	5,46	1,26
7	Lower Skin 7	5,34	1,13
8	Lower Skin 8	5,24	1,01
9	Lower Skin 9	5,15	1,01
10	Lower Skin 10	5,07	1,01
11	Lower Skin 11	4,89	1,01
12	Lower Skin 12	4,65	1,02
13	Lower Skin 13	4,40	1,02
14	Lower Skin 14	4,14	1,02
15	Lower Skin 15	3,87	1,01
16	Lower Skin 16	3,59	1,01
17	Lower Skin 17	3,31	1,02
18	Lower Skin 18	3,01	1,01
19	Lower Skin 19	2,70	1,02
20	Lower Skin 20	2,39	1,02
21	Lower Skin 21	2,06	1,02
22	Lower Skin 22	1,73	1,02
23	Lower Skin 23	1,40	1,02
24	Lower Skin 24	1,07	1,02
25	Lower Skin 25	1,00	1,02
26	Lower Skin 26	1,00	1,02
27	Lower Skin 27	1,00	1,02
28	Lower Skin 28	1,00	1,02

Annex 3 - Numerical results for Part III optimization

Table 8 - Numerical results for the thickness optimization in Sol200 of NACA 2420 profile WB with stress criterion only, in Static Analysis. Front Spar Part II.

Section	Name	Initial Thickness [mm]	Final Thickness [mm]
FRONT SPAR [Part II]			
1	Front Spar 1	3,02	7,43
2	Front Spar 2	2,93	5,93
3	Front Spar 3	2,84	4,36
4	Front Spar 4	2,75	5,02
5	Front Spar 5	2,65	4,85
6	Front Spar 6	2,56	3,32
7	Front Spar 7	2,46	2,82
8	Front Spar 8	2,36	2,50
9	Front Spar 9	2,25	1,84
10	Front Spar 10	2,15	1,00
11	Front Spar 11	2,32	1,00
12	Front Spar 12	2,22	1,00
13	Front Spar 13	2,13	1,15
14	Front Spar 14	2,03	1,47
15	Front Spar 15	1,93	1,51
16	Front Spar 16	1,83	1,68
17	Front Spar 17	1,73	1,58
18	Front Spar 18	1,62	1,70
19	Front Spar 19	1,52	1,85
20	Front Spar 20	1,41	1,76
21	Front Spar 21	1,30	1,47
22	Front Spar 22	1,19	1,37
23	Front Spar 23	1,07	1,18
24	Front Spar 24	1,00	1,01
25	Front Spar 25	1,00	1,00
26	Front Spar 26	1,00	1,00
27	Front Spar 27	1,00	1,00
28	Front Spar 28	1,00	1,00

Table 9 - Numerical results for the thickness optimization in Sol200 of NACA 2420 profile WB with stress criterion only, in Static Analysis. Rear Spar Part II.

Section	Name	Initial Thickness [mm]	Final Thickness [mm]
REAR SPAR			
1	Rear Spar 1	2,60	74,36
2	Rear Spar 2	2,53	75,91
3	Rear Spar 3	2,46	67,46
4	Rear Spar 4	2,39	61,74
5	Rear Spar 5	2,32	65,54
6	Rear Spar 6	2,25	55,26
7	Rear Spar 7	2,18	53,68
8	Rear Spar 8	2,10	47,10
9	Rear Spar 9	2,03	46,08
10	Rear Spar 10	1,95	45,19
11	Rear Spar 11	2,01	41,43
12	Rear Spar 12	1,94	38,75
13	Rear Spar 13	1,86	26,13
14	Rear Spar 14	1,77	25,83
15	Rear Spar 15	1,69	24,13
16	Rear Spar 16	1,61	19,56
17	Rear Spar 17	1,52	15,88
18	Rear Spar 18	1,43	13,82
19	Rear Spar 19	1,34	11,71
20	Rear Spar 20	1,25	8,42
21	Rear Spar 21	1,15	7,08
22	Rear Spar 22	1,05	4,86
23	Rear Spar 23	1,00	2,76
24	Rear Spar 24	1,00	1,83
25	Rear Spar 25	1,00	1,00
26	Rear Spar 26	1,00	1,00
27	Rear Spar 27	1,00	1,00
28	Rear Spar 28	1,00	1,00

Table 10 - Numerical results for the thickness optimization in Sol200 of NACA 2420 profile WB with stress criterion only, in Static Analysis. Upper Skin Part II.

Section	Name	Initial Thickness [mm]	Final Thickness [mm]
UPPER SKIN			
1	Upper Skin 1	5,43	5,35
2	Upper Skin 2	5,28	3,53
3	Upper Skin 3	5,14	3,69
4	Upper Skin 4	4,99	4,22
5	Upper Skin 5	4,85	3,50
6	Upper Skin 6	4,70	3,85
7	Upper Skin 7	4,56	3,01
8	Upper Skin 8	4,42	2,99
9	Upper Skin 9	4,28	2,51
10	Upper Skin 10	4,14	1,97
11	Upper Skin 11	3,98	1,73
12	Upper Skin 12	3,80	1,00
13	Upper Skin 13	3,62	1,01
14	Upper Skin 14	3,44	1,00
15	Upper Skin 15	3,25	1,00
16	Upper Skin 16	3,06	1,00
17	Upper Skin 17	2,87	1,00
18	Upper Skin 18	2,67	1,00
19	Upper Skin 19	2,47	1,00
20	Upper Skin 20	2,26	1,00
21	Upper Skin 21	2,06	1,00
22	Upper Skin 22	1,84	1,00
23	Upper Skin 23	1,62	1,00
24	Upper Skin 24	1,40	1,00
25	Upper Skin 25	1,16	1,00
26	Upper Skin 26	1,00	1,00
27	Upper Skin 27	1,00	1,00
28	Upper Skin 28	1,00	1,00

Table 11 - Numerical results for the thickness optimization in Sol200 of NACA 2420 profile WB with stress criterion only, in Static Analysis. Lower Skin Part II.

Section	Name	Initial Thickness [mm]	Final Thickness [mm]
LOWER SKIN			
1	Lower Skin 1	6,08	3,02
2	Lower Skin 2	5,95	2,88
3	Lower Skin 3	5,82	2,01
4	Lower Skin 4	5,70	2,20
5	Lower Skin 5	5,58	1,73
6	Lower Skin 6	5,46	1,26
7	Lower Skin 7	5,34	1,13
8	Lower Skin 8	5,24	1,01
9	Lower Skin 9	5,15	1,01
10	Lower Skin 10	5,07	1,01
11	Lower Skin 11	4,89	1,01
12	Lower Skin 12	4,65	1,02
13	Lower Skin 13	4,40	1,02
14	Lower Skin 14	4,14	1,02
15	Lower Skin 15	3,87	1,01
16	Lower Skin 16	3,59	1,01
17	Lower Skin 17	3,31	1,02
18	Lower Skin 18	3,01	1,01
19	Lower Skin 19	2,70	1,02
20	Lower Skin 20	2,39	1,02
21	Lower Skin 21	2,06	1,02
22	Lower Skin 22	1,73	1,02
23	Lower Skin 23	1,40	1,02
24	Lower Skin 24	1,07	1,02
25	Lower Skin 25	1,00	1,02
26	Lower Skin 26	1,00	1,02
27	Lower Skin 27	1,00	1,02
28	Lower Skin 28	1,00	1,02

Annex 4 - How to use this work / Documentation Tutorial

In this tutorial I'll present how all information produced during my internship is organized. This document intends to help finding the most important files and how to use them. During my internship on “Structural Optimization of a Flexible Wing: Parametric Model Approach” at the laboratories of Supaero, I had the opportunity to learn how to use MSC Patran and Nastran, so all my work is based on this two softwares. Note that the version used is the 2007 Release. Everything produced is inside the *Documentation* folder.



It's also extremely important to read and understand the work produced by Erick Assis Lima in his work “Structural Optimization of a Flexible Wing: Reduced Model Approach”, since my study is directly related with his, as we were in the same project. I must remember that this internship had duration of 4 months, so it wasn't possible to give a much deeper analysis about this subject. Hope it will be useful and helps you. Any other doubts don't hesitate to contact me by email at chico.habibmattos@gmail.com or my tutor Prof. Dr. Joseph Morlier, of DMSM ISAE.

Francisco Habib Issa Mattos
Rua B, N° 220 - Bairro Andracel
75113-280 - Anápolis - GO, Brazil
+55 62 33 11 16 54

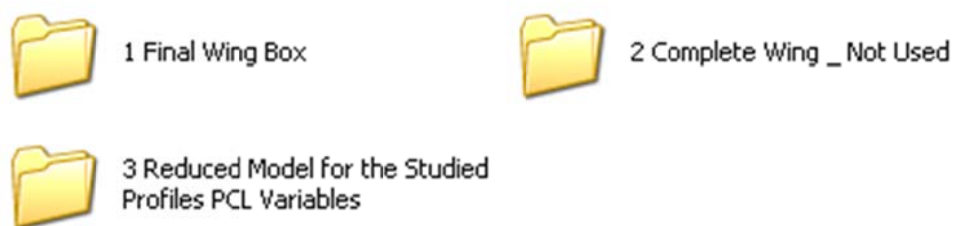
1. Final Report

The final report must be read to understand my work. It explains in logical sequence everything I did as well as why I made some specific decisions about this project. It basically contains all theory I used to accomplish this study, results and a conclusion about the optimization process. It also presents all references used, that could help as well. This version does not contain any confidential information, but is property of the Institut Supérieur de l'Aéronautique et de l'Espace, and must not be replicated without its permission. I also left the final presentation, the one I used to conclude my Projet de Fin d'Etudes at Supaero.



2. Patran PCL Code

The Patran PCL code was created entirely with aid of Microsoft Excel. Look at the *Patran PCL Code/ 1 Final Wing Box* folder. What I did is:



1. Create the geometry in Patran and copy the code written in the .jou file.
2. Insert this piece of code in Excel, respecting all characters and keeping a logical organization
3. I used Excel to replicate the command using its formulas and macros
4. After a copied the final code in Excel to the Text Editor, to substitute the tabulation (□ character at the beginning of each Excel page) for space or any other particularity of

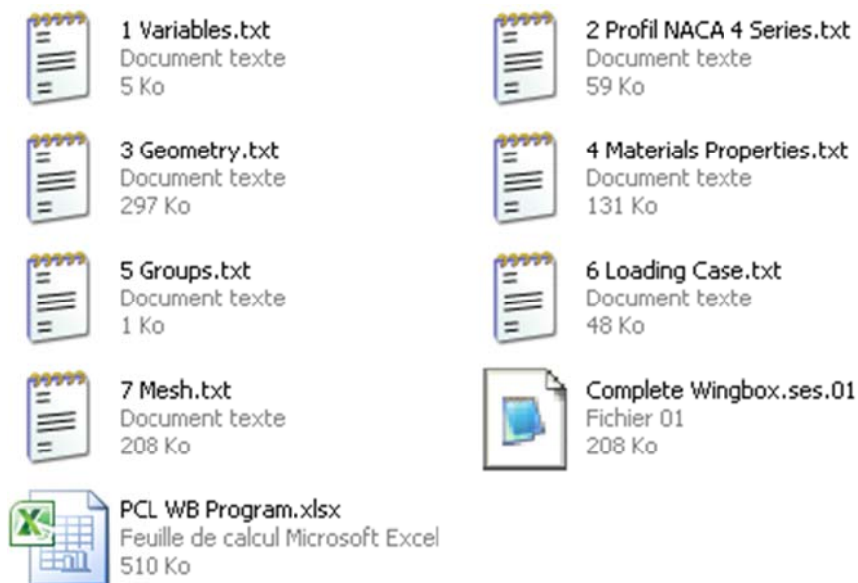
PCL code (for example, “ : ” is not accepted, so its necessary to suppress the space to have “:”)

5. Then I inserted the final code, with text corrections in the session file, and continued the same process.

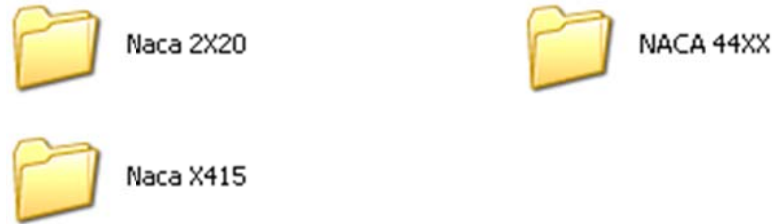
The PCL WB Program in Excel has approximately all code generated that needed big replication. Small steps I did by hand. For more information about the wing creation in Patran, read the Tutorial I created, which is inside the Tutorial Folder.

The final PCL Code was divided in 7 parts:

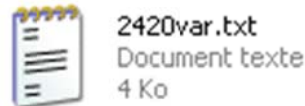
- **1 Variables:** where I declared all variables and inserted the input document *XXXX var.txt* provided by the reduced model (Erick’s work).
- **2 Profil NACA 4 Series:** code that generates all NACA profile.
- **3 Geometry:** all geometry creation, including points, curves and surfaces.
- **4 Material Properties:** creation of all materials and properties, according to the *XXXX var.txt* input.
- **5 Groups:** creation of groups to help visualization.
- **6 Loading Case:** creation of the load case (forces and moments) as well as boundary conditions (cantilever wing)
- **7 Mesh:** creation of all nodes and elements, controlling the entire mesh by *mesh seeds*.



To create a new wing it's necessary to input the desired variables in *1 Variables*. This is the only document that needs to be changed. The other 6 do not need to be touched, unless a change in the meshing is required, so the *7 Mesh* must be re-analyzed. After, copy the text inside the *7 .txt* and copy inside a session file, like the *Complete Wingbox.ses.01*, and run in Patran. It takes approximately 8 minutes to create a new wing.



The folder *2 Complete Wing _ Not Used* has the PCL Code for the entire wing, which includes the external skin and complete rib meshing. In the Inputs from *Reduced Model for the Studied Profiles PCL Variables* folder I left all the *XXXX var.txt* files that I used in my study.



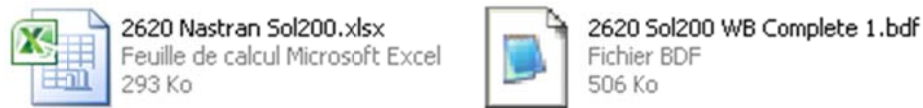
3. Nastran Sol200 Code

The Nastran Sol200 Code was created with aid of Excel as well, the Crimson Editor and the Nastran Quick Reference Guide and Nastran Design Sensitivity and Optimization Users Guide.



3.1 Final Code

The Nastran code has some particularities such as the allowed space to write, limited to 8 bits, as well as the size of a card, limited to 10 tabulation spaces (where each tabulation contains the 8 bits). In this way, Excel is of great help because each cell may correspond directly to 8 bits, and that's why I chose to create all cards of the final code in Excel. To verify the final code, I used the Crimson Editor, which allows a good view of the final code and to check if the cards language constraints are respected. After that, I just copied the code to the *.bdf* file and ran in Nastran.



To be sure that the initial geometry generated by Patran and the initial values given to Nastran in DESVAR were the same, another input code was provided by the Reduced Model in the *XXXX var2.txt* files. This file contains the exactly same thickness of skins and spars that is inside the *XXXX var.txt* files, but in a format that can be directly inserted in the Excel program *Nastran Sol200.xlsx*. This program has all steps used to create the final code in its many pages. The geometrical inputs and thickness must be inserted in the first worksheet (*Table*) near the red cells. After, all calculus will be recomputed, but still some attention must be given to the yellow cells in the *Buckling* page (attention to the order of the exponent). I left an example of NACA 2620 Excel Worksheet and bdf file, and other examples can be found in *Studied Wingbox PCL_SOL200*, inside the *Annexes* folder.

3.2 Crimson Editor 3.72

In the *Crimson Editor 3.72* folder I left the latest version of this program. It's just install and use.



3.3 Inputs from Reduced Model

In the *Inputs from Reduced Model for the Studied Profiles Sol200* folder I left all the *XXXX var2.txt* files that I used in my study.



4. Annexes

In the *Annexes* folder I left my Tutorial PCL Wing Creation, where I show how to create a parametric wing approximately the same way I used to create the studied wing for this project. I did this tutorial in the beginning of my internship, so it's a simple model with quite some differences from the final model, especially in the meshing part and load case. It also doesn't present the NACA profile generation, but is still a good guide.



I also left a folder named *Studied Wingbox PCL_SOL200* where everything about the Patran and Nastran codes relative to each of the 9 studied profiles can be found, such as the final PCL codes, final Sol200 codes as well as the Excel worksheets and some results.

The last thing I left is a program called Camstudio that captures the PC screen image, which I used to create the small video that presents the wing creation. It's a good program if you wish to present something of Patran or Fluent to public, without needing these softwares.

1 Studied Wingbox PCL_SOL200

5. References

In the *References* folder I left organized all the references I used and presented in the final report. Note that they follow the same numeration of the report, which does not mean an importance order. The *Other* folder contains a few more references that were given to me in the beginning of this internship. It's extremely important to also consult the references of Erick's work, since they have a considerably more analytical basis, as well as all information about the reduced model and the plan of experience.

